MACROTRANSPORT PROCESSES IN BRANCHING NETWORKS: MODELING CONVECTIVE-DIFFUSIVE PHENOMENA IN THE LUNG

by
Michelle D. Bryden
B.S., Chemical Engineering
University of California, Davis, 1992

Submitted to the Department of Chemical Engineering
in Partial Fulfillment of the Requirements for the
Degree of

MASTER OF SCIENCE

in Chemical Engineering

at the
Massachusetts Institute of Technology
May 1994

Signature of Author ....
Department of Chemical Engineering
May 3, 1994

Certified by ....
Professor Howard Brenner
Department of Chemical Engineering
Thesis Supervisor

Accepted by ....
Professor Robert Cohen
Graduate Officer
Department of Chemical Engineering

MACROTRANSPORT PROCESSES IN BRANCHING NETWORKS: MODELING CONVECTIVE-DIFFUSIVE PHENOMENA IN THE LUNG

By
Michelle D. Bryden

Submitted to the Department of Chemical Engineering
in Partial Fulfillment of the Requirements for the Degree of
MASTER OF SCIENCE
in Chemical Engineering
at the
Massachusetts Institute of Technology
May 1994

ABSTRACT

This thesis investigates convective-diffusive phenomena in branching networks. While the motivation for this study arose from an interest in modeling transport processes in the lung, the general results of this study are applicable to a large class of transport phenomena occurring in branching systems. This analysis develops a general macrotransport theory for branching systems comparable to that existing for spatially periodic systems, leading to a one-dimensional macrotransport description of transport in branching networks. This work departs from the existing theory for spatially periodic systems in that the macrotransport coefficients are found to vary with position to account for the variation in the mean velocity in the direction of flow. In addition, the macrotransport equation contains an 'apparent velocity' term, present even in the absence of convection, which arises from the increase in cross-sectional area with increasing generation number. It is also shown that the net dispersion is decreased as a consequence of axial gradients in the mean velocity.

Thesis Supervisor: Professor Howard Brenner

Title: Willard H. Dow Professor of Chemical Engineering

ACKNOWLEDGEMENTS

I would like to express my gratitude to Professor Howard Brenner for his helpful guidance and insight, as well as for his many words of encouragement. I would also like to thank my husband, Ken, for his endless support and patience. Thanks also to my parents for their support and to my brother, Jeff, who sparked my interest in mathematics and science at a very young age.

This research was supported by a National Science Foundation Graduate Research Fellowship.

TABLE OF CONTENTS

TABLE OF FIGURES

I. INTRODUCTION

This research investigates convection and dispersion of aerosol or hydrosol particles or dissolved gas species in a branching network such as the lung. As a particle travels through such a branching network, it experiences constantly decreasing velocities, in addition to encountering an increasing amount of area into which it can diffuse laterally. The decreasing velocity and increasing area each affect the overall transport in the branching system, making transport in this type of system very different from transport in constant-area systems such as capillary tubes or porous media.

Understanding transport in the lung is useful for several purposes. Aerosol drug delivery systems, such as those used to treat asthma, depend on the transport of medication inhaled into the lung to be effective. In addition, understanding the transport of particulates in the lung will aid in understanding how airborne pollution affects lung function. Finally, tracer studies are one method used for diagnosis of lung disease. An understanding of how lung geometry affects tracer dispersion will aid in the interpretation of the results of such tests.

Previous researchers have taken several different approaches in modelling dispersion in the lung. Ultmann and Blatman (1978) assume that the results for undeveloped Taylor dispersion in an infinitely long tube apply in each of the lung airways. Federspiel (1988) used a multiscale perturbation technique to study the case of purely diffusive transport. Recently, Edwards (1993) treated the convective-diffusive case by assigning an empirically determined effective dispersion coefficient to each tube and then finding the average velocity and dispersivity for the entire lung, which was treated as one cell of a spatially periodic system.

This work begins with an exact description of transport in a branching array and uses the methods of macrotransport theory to determine the mean particle velocity and dispersivity as a function of axial position in the branching network. The methods used are similar to those which have been developed for spatially periodic systems (Brenner and Edwards, 1993), with provision made for the increasing area and decreasing velocity experienced by a particle as it moves further into the system. Thus, the result is a one dimensional equation with axially-varying coefficients, which can be solved to find the average concentration of particles as a function of time and axial position.

II. THEORY

1. TRANSPORT IN THE BRANCHING NETWORK

1.1 Geometry

This work models transport in a system of 'branching' cells, as shown in Figure 1. In this model, the branching system consists of an infinite number of generations, each containing 2^n cells, where n is the generation number. Each of these cells may be identified by a pair of integer indices, (n, j). The first index, n, is the generation number, and takes on the values 0, 1, 2, ..., ∞. The value $n = 0$ is assigned to the generation at the entrance to the network, which consists of a single cell. The second index, j, the intragenerational index, takes on the values 1, 2, ..., 2^n. In this numbering system, the two 'exit' faces of cell $\{n, j\}$ are connected to the 'entrance' faces of cells $\{n+1, 2j-1\}$ and

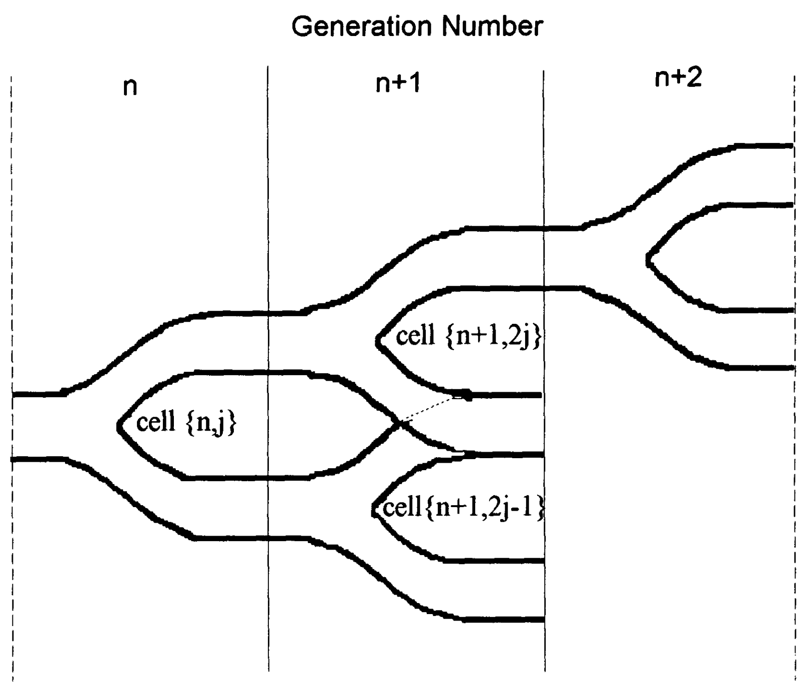

FIGURE 1: Interior portion of a branching array

$\{n+1, 2j\}$. In this paper, the term 'entrance face' will be used to refer to the face of the unit cell closest to the zeroth generation, while 'exit face' will be used for either of the two faces on the opposite side of the cell.

In the subsequent analysis, the cells are regarded as being geometrically identical, both intra- and intergenerationally. Each of the cells $\{n, j\}$ encloses a volumetric domain, $V\{n, j\}$ of volume V, within its boundaries, $\partial V\{n, j\}$, as shown in Figure 2. The solid surfaces are denoted $S_s\{n, j\}$, while the inlet and exit faces are represented by $S_i\{n, j\}$ and $S_e\{n, j\}$, respectively. A directed surface element $d\mathbf{S}$ may be written as $d\mathbf{S} = \nu\, dS$, where ν is the outwardly-directed unit normal to the surface.

The infinite, fluid-filled domain will be denoted by $V_\infty = \sum_n \sum_j V\{n, j\}$. The surface, ∂V_∞ constituting the system's boundaries is comprised of: (i) the solid surfaces forming the walls of the entire system, $\sum_n \sum_j S_s\{n, j\}$; (ii) the inlet surface of the network, $S_i\{0,1\}$; and (iii) the exit boundaries, $\sum_j S_e\{\infty, j\}$, at the infinite 'end' of the network. Explicitly,

$$\partial V_\infty = \sum_n \sum_j S_s\{n, j\} \oplus S_i\{0,1\} \oplus \sum_j S_e\{\infty, j\} . \tag{1}$$

A position vector within the infinite system will be represented by $\mathbf{R}$. Alternatively, this position may be represented by

$$\mathbf{R} = \mathbf{R}_{n,j} + \mathbf{r}, \tag{2}$$

where the discrete vector, $\mathbf{R}_{n,j}$ is the position vector identifying cell $\{n, j\}$ (say, its centroid) and $\mathbf{r}$ is a local position vector, $\mathbf{r} \in V\{n, j\}$, measured from an origin located at $\mathbf{R}_{n,j}$. As shown in Figure 2, the vector 'length' of a cell is denoted $\mathbf{l}$, while the

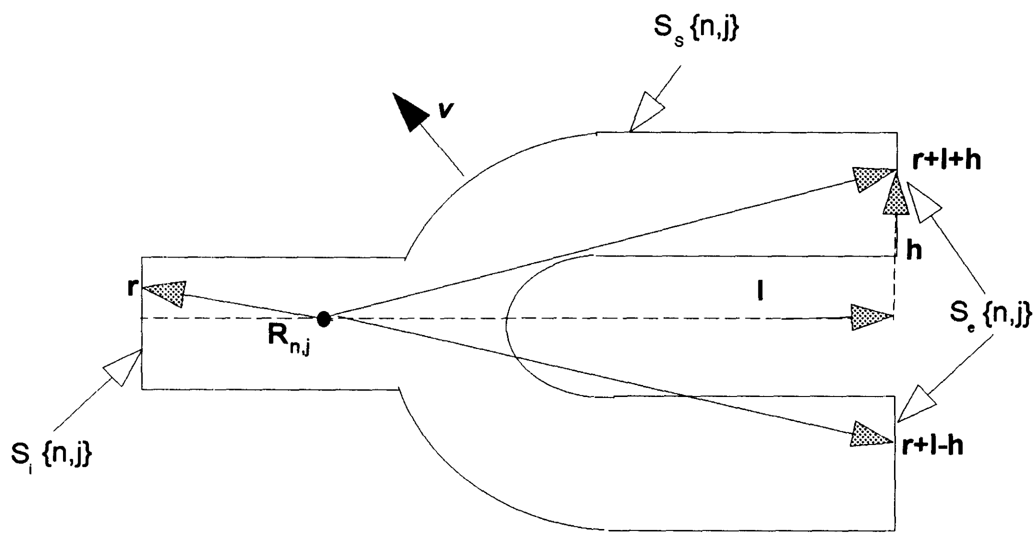

FIGURE 2: Unit cell

'branching height', or the vector distance from the centerline of the unit cell to the center of the upper exit face of the cell, is given by the vector $\mathbf{h}$. Points lying on the exit surfaces, $S_e\{n, j\}$, of cell $\{n, j\}$ lie simultaneously on the inlet surface of one of the cells $\{n+1, 2j\}$ or $\{n+1, 2j-1\}$. Consequently, within our notational system, the point $\mathbf{R}_{n, j} + (\mathbf{r} + \mathbf{l} + \mathbf{h})$, which lies on the upper exit surface of cell $\{n, j\}$, is geometrically coincident with the point $\mathbf{R}_{n+1, 2j} + \mathbf{r}$, lying on the entry face to cell $\{n+1, 2j\}$. Likewise, the point $\mathbf{R}_{n, j} + (\mathbf{r} + \mathbf{l} - \mathbf{h})$, located on the lower exit surface of cell $\{n, j\}$, coincides with the point $\mathbf{R}_{n+1, 2j-1} + \mathbf{r}$ on the entry face of cell $\{n+1, 2j-1\}$.

1.2 Kinematics of Fluid Flow in Branching Systems

The velocity field, $\mathbf{v} \equiv \mathbf{v}\{n, j; \mathbf{r}\}$ in a branching system is a function of both local position, $\mathbf{r}$, and global (or cellular) position $\{n, j\}$. On the solid boundaries of the system, the no-slip condition requires that:

$$\mathbf{v} = \mathbf{0} \quad \text{on} \quad S_B. \tag{3}$$

Due to symmetry, the velocity field is identical within every cell, j, of a given generation, n. That is,

$$\mathbf{v} \equiv \mathbf{v}(n; \mathbf{r}), \tag{4}$$

independently of j. The velocity field, however, will vary from one generation to another. For an incompressible fluid, the volumetric flow rate, q, through the system is an invariant. The increase in the number of cells per generation thus causes a decrease in the average velocity in each generation, defined as:

$$\overline{\mathbf{v}_n} = \frac{1}{V}\int_{V\{n,j\}} \mathbf{v}(n;\mathbf{r})\, d^3\mathbf{r}, \tag{5}$$

where $d^3\mathbf{r}$ is an infinitesimal volume element centered at **r**. As a result of the invariance of the volumetric flow rate, the average velocity in each generation must be such that

$$\overline{\mathbf{v}_n} = \frac{\overline{\mathbf{v}_0}}{2^n}, \tag{6}$$

where $\overline{\mathbf{v}}_0$ is the average velocity in the zeroth generation of the system.

Consider the class of self-similar flows for which

$$\mathbf{v}(n;\mathbf{r}) = 2^{-n}\mathbf{U}(\mathbf{r}). \tag{7}$$

Here,

$$\mathbf{U}(\mathbf{r}) = \mathbf{v}(0;\mathbf{r}). \tag{8}$$

This relation implies that the normalized velocity profile is the same in all cells of the system. Examples of such self-similar flows are incompressible potential flows or creeping flows. In order for the velocity to remain continuous throughout the system, **U** must be a function such that

$$\mathbf{U}(\mathbf{r}) = 2\mathbf{U}(\mathbf{r}+\mathbf{l}\pm\mathbf{h}). \tag{9}$$

In words, the velocity at a point on the 'entry' face of the cell is twice as large as that at the equivalent point on the 'exit' face.

1.3 Conditional Probability Density

Suppose that at time $t = 0$, an effectively point-sized Brownian tracer particle is instantaneously introduced into the network at a point $\mathbf{R}'$. In applications, the Brownian tracer is identified with a sub-micron aerosol or hydrosol particle suspended in the flowing fluid. Let $P(\mathbf{R},t\,|\,\mathbf{R}')$ denote the conditional probability density that the tracer is located at point $\mathbf{R}$ at time t, given that it was located at point $\mathbf{R}'$ at time $t = 0$. Conservation of probability density dictates that

$$\frac{\partial P}{\partial t} + \nabla\cdot\mathbf{J} = \delta(\mathbf{R}-\mathbf{R}')\,\delta(t)\,, \qquad (10)$$

where $\mathbf{J}$ is the flux of probability density relative to a stationary observer, $\nabla = \partial/\partial\mathbf{R}$ is the gradient operator, and δ is the Dirac delta function. The flux vector $\mathbf{J}$ is given by a constitutive equation of the form

$$\mathbf{J}(\mathbf{R},\, t|\mathbf{R}') = \mathbf{V}(\mathbf{R})\,P - D\nabla P, \qquad (11)$$

where D (assumed constant) is the diffusivity of the tracer.

The probability density is determined by Eqs. (10) and (11) in conjunction with appropriate boundary conditions. Firstly, the solid surfaces of the network are assumed impermeable to both the tracer and the solvent, therefore

$$\mathbf{v}\cdot\mathbf{J} = 0 \quad \text{on } S_s. \qquad (12)$$

As a consequence of Eqs. (3) and (11), this is equivalent to

$$\mathbf{v}\cdot\nabla P = 0 \quad \text{on } S_s. \qquad (13)$$

In addition, the condition that the particle does not exit the network requires that

$$\boldsymbol{\nu}\cdot\mathbf{J} = 0 \quad \text{on} \quad S_i\{0,1\}, \tag{14}$$

i.e.

$$\boldsymbol{\nu}\cdot(\mathbf{U}P - D\nabla P) = 0 \quad \text{on} \quad S_i\{0,1\}, \tag{15}$$

and that

$$P \to 0 \text{ as } \mathbf{R} \to \infty. \tag{16}$$

To demonstrate conservation of probability within the network, integrate Eq. (10) over the entire domain (V_∞) to obtain:

$$\frac{d}{dt}\int_{V_\infty} P d^3\mathbf{R} = -\int_{V_\infty} \nabla\cdot\mathbf{J} d^3\mathbf{R} + \delta(t), \tag{17}$$

where we have used the identity

$$\int_{V_\infty} \delta(\mathbf{R} - \mathbf{R}') d^3\mathbf{R} = 1. \tag{18}$$

Use of the divergence theorem yields:

$$\frac{d}{dt}\int_{V_\infty} P d^3\mathbf{R} = -\int_{\partial V_\infty} d\mathbf{S}\cdot\mathbf{J} + \delta(t). \tag{19}$$

As a consequence of (12), (15), and (16), the surface integral in (19) vanishes over each of the subdomains in (1). Equation (19) therefore becomes:

$$\frac{d}{dt}\int_{V_\infty} P d^3\mathbf{R} = \delta(t). \tag{20}$$

Integrating this expression with respect to time yields:

$$\int_{V_\infty} P d^3\mathbf{R} = \mathrm{H}(t)\,, \tag{21}$$

where H(t) is the Heaviside step function,

$$\mathrm{H}(t) = \begin{cases} 1 & t > 0 \\ 0 & t < 0 \end{cases} . \tag{22}$$

Thus, for times less than zero, there is zero probability of the particle being located within the network, whereas for times greater than zero, the probability is identically unity.

1.4 Intracellular Probability Density

The conditional probability density may be regarded as being functionally of the form:

$$P^{n,j} \equiv P^{n,j}(n, j, \mathbf{r}, t \,|\, n', j', \mathbf{r}') \overset{def}{=} P(\mathbf{R}, t \,|\, \mathbf{R}')\,. \tag{23}$$

Here, $P^{n,j}$ is the intracellular probability density at point $\mathbf{r}$ within the j^{th} cell of the n^{th} generation. Transport within a given cell is governed by the conservation equation:

$$\frac{\partial P^{n,j}}{\partial t} + \nabla\cdot\mathbf{J}^{n,j} = \delta_{nn'}\delta_{jj'}\delta(\mathbf{r}-\mathbf{r}')\,\delta(t)\,, \tag{24}$$

where δ_{kl} is the Kronecker delta ($\delta_{kl} = 1$ for k = l and 0 for k $\neq$ l). The flux, $\mathbf{J}^{n,j}$ within that cell is given by the constitutive equation:

$$\mathbf{J}^{n,j} = 2^{-n}\mathbf{U}(\mathbf{r})\,P^{n,j} - D\nabla P^{n,j}. \tag{25}$$

Boundary conditions at the inlet and exit of cell $\{n, j\}$ may be found by imposing conditions of continuity of probability density and flux between contiguous generations.

The former is represented by

$$P^{n,j}(\mathbf{r}+\mathbf{l}\pm\mathbf{h}) = P^{n+1,\,2j(-1)}(\mathbf{r}), \tag{26}$$

while the later is given by

$$\mathbf{J}^{n,j}(\mathbf{r}+\mathbf{l}\pm\mathbf{h}) = \mathbf{J}^{n+1,2j(-1)}(\mathbf{r}). \tag{27}$$

Here, the additional arguments, t, n, j, n', j', and $\mathbf{r}'$, that would otherwise have explicitly appeared in these relations have been suppressed for emphasis. Note that each of these boundary conditions represents conditions on two different boundaries, namely the 'upper' and 'lower' exit faces of the cell. Here, the '+' sign in the '±' operator is associated with the $2j$ cell of generation n+1, while the '-' sign corresponds to the $2j$-1 cell of that generation. Equations (25), (26), and (27) combine to give a boundary condition on the gradient of the probability density:

$$\nabla P^{n,j}(\mathbf{r}+\mathbf{l}\pm\mathbf{h}) = \nabla P^{n+1,2j(-1)}(\mathbf{r}). \tag{28}$$

The condition of no flux through the solid surfaces of the system requires that

$$\mathbf{v}\cdot\nabla P^{n,j} = 0 \quad \text{on } S_g\{n,j\}, \tag{29}$$

An additional boundary condition is needed for the cell at the entrance to the network, cell {0,1}, as its inlet face, $S_i\{0,1\}$, does not connect to another cell. In this cell, Eq. (15) requires that

$$\mathbf{v}\cdot(\mathbf{U}P^{0,1} - D\nabla P^{0,1}) = 0 \qquad \text{on } S_i\{0,1\}. \tag{30}$$

In addition, for large n, (16) requires that

$$P^{n,j} \to 0 \quad \text{as } n \to \infty \qquad \forall (j, \mathbf{r}) . \tag{31}$$

1.5 Generational Probability Density

Inasmuch as all of the cells of the branching array are geometrically identical and the phenomenological coefficients governing the transport equation are independent of intragenerational position, j, the later represents a 'dead' degree of freedom. We therefore define the conditional generational probability, P^n:

$$P^n(n, \mathbf{r}, t | n', j', \mathbf{r}') = \sum_{j=1}^{2^n} P^{n,j}(n, j, \mathbf{r}, t | n', j', \mathbf{r}') . \tag{32}$$

Summing Eqs. (24) - (26), (28) and (29) from $j = 1$ to 2^n generates the boundary-value problems for each of the generational probabilities:

$$\frac{\partial P^n}{dt} + \nabla \cdot \mathbf{J}^n = \delta_{nn'} \delta(\mathbf{r} - \mathbf{r}') \delta(t) , \tag{33}$$

$$\mathbf{J}^n = 2^{-n} \mathbf{U}(\mathbf{r}) P^n - D \nabla P^n \tag{34}$$

$$\mathbf{v} \cdot \nabla P^n = 0 \quad \text{on } S_s , \tag{35}$$

$$P^n(\mathbf{r} + \mathbf{l} + \mathbf{h}) + P^n(\mathbf{r} + \mathbf{l} - \mathbf{h}) = P^{n+1}(\mathbf{r}) \tag{36}$$

$$\nabla P^n(\mathbf{r} + \mathbf{l} + \mathbf{h}) + \nabla P^n(\mathbf{r} + \mathbf{l} - \mathbf{h}) = \nabla P^{n+1}(\mathbf{r}) \tag{37}$$

An additional boundary condition is needed on the inlet face of the zeroth generation:

$$\mathbf{v} \cdot (\mathbf{U} P^0 - D \nabla P^0) = 0 \qquad \text{on } S_i\{0, 1\}. \tag{38}$$

For large n, Eq. (31) requires that

$$P^n \to 0 \quad \text{as } n \to \infty. \tag{39}$$

2. MOMENTS OF THE PROBABILITY DISTRIBUTION

Define the m^{th} - order local moments (m = 0, 1, 2, ...)

$$\mathbf{P}_m(\mathbf{r}, t \mid n', j', \mathbf{r}') = \sum_{n=0}^{\infty} (\mathbf{R}_n - \mathbf{R}'_n)^m P^n(n, \mathbf{r}, t \mid n', j', \mathbf{r}'), \tag{40}$$

where

$$\mathbf{R}_n = n\mathbf{l}, \tag{41}$$

and the m^{th}- order total moments

$$\mathbf{M}_m(t \mid n', j', \mathbf{r}') = \int_V \mathbf{P}_m(\mathbf{r}, t \mid n', j', \mathbf{r}')\, d^3\mathbf{r}. \tag{42}$$

Each of the total moments possesses a different physical interpretation, which reveals information about the behavior of the system as a whole. The zeroth total moment, M_0, represents the total conditional probability of finding the tracer particle somewhere within the network at time t, given that it was introduced into the system at the position $\mathbf{R}' = \mathbf{R}'_{n,j} + \mathbf{r}'$ at time $t = 0$. Likewise, the first total moment, $\mathbf{M}_1$, is the average displacement of the particle at time t from its original position. The spread in the distribution is directly related to the second centered moment, $(\mathbf{M}_2 - \mathbf{M}_1\mathbf{M}_1)$.

Define also the m^{th} local and total α - *weighted* moments (m = 0, 1, ..., α = 0, 1, ...)

$$\mathbf{P}_m^{[\alpha]}(\mathbf{r}, t \mid n', j', \mathbf{r}') = \sum_{n=0}^{\infty} 2^{-\alpha n} (\mathbf{R}_n - \mathbf{R}'_n)^m P^n(n, \mathbf{r}, t \mid n', j', \mathbf{r}'), \tag{43}$$

and

$$\mathbf{M}_m^{[\alpha]}(t \mid n', j', \mathbf{r}') = \int_V \mathbf{P}_m^{[\alpha]}(\mathbf{r}, t \mid n', j', \mathbf{r}')\, d^3\mathbf{r}. \tag{44}$$

Our attention will be primarily focused on the $\alpha = 0$ and $\alpha = 1$ moments. The $\alpha = 0$ moments are identical to the unweighted moments defined in (40) and (42) which involve the total probability of the particle being in anywhere in each generation. In contrast, when the probability is independent of j, the $\alpha = 1$ moments are equivalent to including only the probability of the particle being in any *one* of the 2^n cells in each generation.

The governing equations for $\mathbf{P}_m^{[\alpha]}$ can be found by multiplying (33) by $2^{-\alpha n}(\mathbf{R}_n - \mathbf{R}'_n)^m$ and summing over all n to obtain

$$\frac{\partial \mathbf{P}_m^{[\alpha]}}{dt} + \nabla \cdot \mathbf{J}_m^{[\alpha]} = \delta_{m0} 2^{-\alpha n'} \delta(\mathbf{r} - \mathbf{r}') \delta(t) , \tag{45}$$

where

$$\mathbf{J}_m^{[\alpha]} = \mathbf{U}(\mathbf{r}) \mathbf{P}_m^{[\alpha+1]} - D\nabla \mathbf{P}_m^{[\alpha]} , \tag{46}$$

and in which the source term appearing on the right-hand side of Eq. (45) arises from use of the identity

$$\sum_{n=0}^{\infty} \delta_{nn'} f(n) = f(n') . \tag{47}$$

These equations are to be solved in conjunction with the boundary condition

$$\mathbf{v} \cdot \nabla \mathbf{P}_m^{[\alpha]} = \mathbf{0} \text{ on } S_s . \tag{48}$$

Boundary conditions are also needed on each of the cell faces. These are obtained by multiplying Eqs. (36) and (37) by $2^{-\alpha n}(\mathbf{R}_n - \mathbf{R}'_n)^m$ and summing over all n. As shown in Appendix A, the boundary conditions derived in this manner can be expressed in terms of the 'branching jump' operator, $\Vert \ldots \Vert$, defined as the difference between the sum of the values of a function at a pair of equivalent points on the two exit faces of the cell and the value of this function at the equivalent point on the inlet face. Explicitly, for any scalar, vector, or tensor-valued function **f**,

$$\|\mathbf{f}\| \stackrel{def}{=} 2\mathbf{f}(\mathbf{r}+\mathbf{l}\pm\mathbf{h}) - \mathbf{f}(\mathbf{r})\,. \tag{49}$$

For asymptotically long times, the boundary conditions on the $\alpha = 0$ moments are

$$\|P_0\| \simeq 0, \tag{50}$$

$$\|\nabla P_0\| \simeq 0, \tag{51}$$

$$\|\mathbf{P}_1\| \simeq -\|\mathbf{z}P_0\|, \tag{52}$$

$$\|\nabla\mathbf{P}_1\| \simeq -\|\nabla(\mathbf{z}P_0)\|, \tag{53}$$

$$\|\mathbf{P}_2\| \simeq \left\|\frac{\mathbf{P}_1\mathbf{P}_1}{P_0}\right\|, \tag{54}$$

$$\|\nabla\mathbf{P}_2\| \simeq \left\|\nabla\left(\frac{\mathbf{P}_1\mathbf{P}_1}{P_0}\right)\right\|, \tag{55}$$

whereas for $\alpha = 1$, the requisite jump boundary conditions are

$$\|\mathbf{U}P_0^{[1]}\| \simeq 0, \tag{56}$$

$$\|\mathbf{U}\nabla P_0^{[1]}\| \simeq 0, \tag{57}$$

$$\|\mathbf{U}\mathbf{P}_1^{[1]}\| \simeq -\|\mathbf{U}\mathbf{z}P_0^{[1]}\|, \tag{58}$$

$$\|\mathbf{U}\nabla\mathbf{P}_1^{[1]}\| \simeq -\|\mathbf{U}\nabla(\mathbf{z}P_0^{[1]})\|, \tag{59}$$

$$\|\mathbf{U}\mathbf{P}_2^{[1]}\| \simeq \left\|\mathbf{U}\frac{\mathbf{P}_1^{[1]}\mathbf{P}_1^{[1]}}{P_0^{[1]}}\right\|, \tag{60}$$

$$\|\mathbf{U}\nabla\mathbf{P}_2^{[1]}\| \simeq \left\|\mathbf{U}\nabla\left(\frac{\mathbf{P}_1^{[1]}\mathbf{P}_1^{[1]}}{P_0^{[1]}}\right)\right\|. \tag{61}$$

Here, **z** is the axial component of the position vector.

From the above differential equations and boundary conditions governing the local moments, $\mathbf{P}_m^{[\alpha]}$, one can determine the time rate-of-change of the total moments, $\mathbf{M}_m$. Integrating (45) with $\alpha = 0$ over the volumetric domain, V, of a unit cell gives

$$\frac{d\mathbf{M}_m}{dt} = \frac{d}{dt}\int_V \mathbf{P}_m d^3\mathbf{r} = -\int_V \nabla\cdot\mathbf{J}_m d^3\mathbf{r} + \delta_{m0}\delta(t)\,. \tag{62}$$

Applying the divergence theorem to the integral on the right yields

$$\frac{d\mathbf{M}_m}{dt} = -\int_{\partial V} d\mathbf{S}\cdot\mathbf{J}_m + \delta_{m0}\delta(t)\,. \tag{63}$$

Since $\nu\cdot\mathbf{J}_m = 0$ on the solid surfaces, S_s, of the cell, it follows that

$$\int_{\partial V} d\mathbf{S}\cdot\mathbf{J}_m = \int_{S_e} d\mathbf{S}\cdot\|\mathbf{J}_m\|, \tag{64}$$

where S_e is either of the two exit faces. The jump in the flux is

$$\|\mathbf{J}_m\| = \|\mathbf{U}\mathbf{P}_m^{[1]}\| - D\|\nabla\mathbf{P}_m\|\,. \tag{65}$$

Examination of the latter in light of Eqs. (50) - (61) reveals that for a specified m, $\|\mathbf{J}_m\|$ can be expressed entirely in terms of lower-order local moments $\mathbf{P}_{m-1}^{[\alpha]}$, $\mathbf{P}_{m-2}^{[\alpha]}$, ... $\mathbf{P}_1^{[\alpha]}$, $\mathrm{P}_0^{[\alpha]}$ $(\alpha = 0, 1)$. Thus, in order to calculate the time rates-of-change of the total moments, $\mathbf{M}_m$ of a given rank m, it suffices to determine only the local moments of rank less than m.

2.1 Zeroth-Order Moments:

Equations (45) and (46) with $m = 0$ furnish the governing equations for the zeroth moments ($\alpha = 0, 1, \ldots$)

$$\frac{\partial P_0^{[\alpha]}}{\partial t} + \nabla\cdot\mathbf{J}_0^{[\alpha+1]} = 2^{-\alpha n}\delta(\mathbf{r} - \mathbf{r}')\delta(t)\,, \tag{66}$$

$$\mathbf{J}_0^{[\alpha]} = \mathbf{U}(\mathbf{r})P_0^{[\alpha+1]} - D\nabla P_0^{[\alpha]}\,. \tag{67}$$

These equations are to be solved in conjunction with the boundary conditions (50), (51), (56), and (57).

Set $m = 0$ in Eqs. (63) - (65) to obtain

$$\frac{dM_0}{dt} = \int_{S_e} d\mathbf{S}\cdot(-\|\mathbf{U}P_0^{[1]}\| + D\|\nabla P_0\|) + \delta(t)\,. \tag{68}$$

In conjunction with (51) and (56) integration of the above expression yields

$$M_0 = \mathrm{H}(t)\,. \tag{69}$$

The probability of the particle being somewhere in the system is thus always identically unity for $t > 0$. This result is consistent with Eq. (21), since

$$\begin{aligned} M_0 &= \int_V \sum_{n=0}^{\infty} P^n d^3\mathbf{r} \\ &= \int_V \sum_{n=0}^{\infty} \sum_{j=1}^{2^n} P^{n,j} d^3\mathbf{r} \\ &= \int_{V_\infty} P d^3\mathbf{R}\,. \end{aligned} \tag{70}$$

Recasting (66) in dimensionless form gives

$$\frac{\partial P_0^{[\alpha]}}{\partial T} + \mathrm{Pe}\,\mathbf{u}\cdot\nabla P_0^{[\alpha+1]} - \nabla^2 P_0^{[\alpha]} = \frac{l^2}{D} 2^{-\alpha n} \delta(\mathbf{r}-\mathbf{r}')\,\delta(t)\,, \tag{71}$$

where

$$T \overset{def}{=} \frac{t l^2}{D}, \quad \mathrm{Pe} \overset{def}{=} \frac{\bar{U} l}{D}, \tag{72a,b}$$

$$\mathbf{u}(\mathbf{r}) \overset{def}{=} \frac{\mathbf{U}(\mathbf{r})}{\bar{U}}, \tag{72c}$$

$$\bar{U} \overset{def}{=} \frac{1}{V}\int_V \mathbf{i}_x\cdot\mathbf{U}(\mathbf{r})\, d^3\mathbf{r}\,. \tag{72d}$$

Consider Eq.(71) with $\alpha = 1$. Let $P_0^{[1]}$ be expressed as

$$P_0^{[1]}(\mathbf{r}, t\,|n', j', \mathbf{r}') = \frac{1}{V} M_0^{[1]}(t\,|n', j', \mathbf{r}') + \wp_0^{[1]}(\mathbf{r}, t\,|n', j', \mathbf{r}')\,, \tag{73}$$

where $\wp_0^{[1]}$ contains all of the spatial variation of $P_0^{[1]}$. Integration of the above over the unit cell shows that

$$\int_V \wp_0^{[1]}(\mathbf{r}, t\,|n', j', \mathbf{r}')\, d^3\mathbf{r} = 0\,. \tag{74}$$

Substitution of (73) into the governing equation (71) for $P_0^{[1]}$ gives

$$\frac{dM_0^{[1]}}{dT} + \frac{\partial \wp_0^{[1]}}{\partial T} + \mathrm{Pe}\,\mathbf{u}\cdot\nabla P_0^{[2]} - \nabla^2 \wp_0^{[1]} = \frac{l^2}{D} 2^{-n} \delta(\mathbf{r}-\mathbf{r}')\,\delta(t)\,, \tag{75}$$

subject to the boundary conditions

$$\wp_0^{[1]}(\mathbf{r}) = \wp_0^{[1]}(\mathbf{r}+\mathbf{l}\pm\mathbf{h})\,, \tag{76}$$

$$\nabla\wp_0^{[1]}(\mathbf{r}) = \nabla\wp_0^{[1]}(\mathbf{r}+\mathbf{l}\pm\mathbf{h})\,. \tag{77}$$

(These boundary conditions are equivalent to those stated in (56)- (57)). For the case in which Pe = 0, $\wp_0^{[1]}$ decays asymptotically with time, so that for long times

$$P_0^{[1]}(\mathbf{r},t|n',j',\mathbf{r}') \approx \frac{1}{V}M_0^{[1]}(t|n',j',\mathbf{r}') \qquad \textbf{(78)}$$

For long times, therefore, any spatial variation in $P_0^{[1]}$ is a result of the nonhomogeneous term, $Pe\mathbf{u}\cdot\nabla P_0^{[2]}$. Thus, $\wp_0^{[1]}$ must be the proportional to this convective term. For long times, $P_0^{[1]}$ may be replaced by (78) if

$$\frac{M_0^{[1]}}{V} >> PeP_0^{[2]} \qquad \textbf{(79)}$$

or, equivalently,

$$Pe << \frac{M_0^{[1]}}{M_0^{[2]}}. \qquad \textbf{(80)}$$

We make the *a posteriori* assumption that the latter criterion is satisfied. $P_0^{[1]}$ may therefore be approximated by (78), indicating that $P_0^{[1]}$ is independent of position **r** within the cell. Ultimately, the solution of the macrotransport equation will show that $M_0^{[2]}$ decays more rapidly than $M_0^{[1]}$, so that for all times greater than some T » 1, this assumption is valid. (See Appendix C for verification of this assumption.)

For long times, P_0 assumes the form

$$P_0 \approx P_0^\infty + \exp, \qquad \textbf{(81)}$$

where 'exp' denotes terms in **r**, t, and **r**$'$ which decay exponentially with time and $P_0^\infty(\mathbf{r})$ is governed by

$$\nabla^2 P_0^\infty = 0, \qquad \textbf{(82)}$$

$$\mathbf{v}\cdot\nabla P_0^\infty = 0 \quad \text{on } S_s, \qquad \textbf{(83)}$$

$$\|P_0^\infty\| = 0, \tag{84}$$

$$\|\nabla P_0^\infty\| = 0. \tag{85}$$

In order for this problem to be completely specified, the normalization condition is needed

$$\int_V P_0^\infty d^3\mathbf{r} = 1. \tag{86}$$

This condition retains the unit normalization information originally contained in the source term in (66), which has been lost in the steady-state formulation of the P_0^∞ problem.

2.2 First Order Moments

In order to find the first unweighted moment, set $m = 1$ and $\alpha = 0$ in Eqs. (45) and (46) and use the boundary conditions (48), (52), and (53)

$$\frac{\partial \mathbf{P}_1}{\partial t} + \nabla\cdot\mathbf{J}_1 = 0, \tag{87}$$

$$\mathbf{J}_1 = \mathbf{U}(\mathbf{r})\mathbf{P}_1^{[1]} - D\nabla\mathbf{P}_1, \tag{88}$$

$$\mathbf{v}\cdot\nabla\mathbf{P}_1 = 0 \quad \text{on } S_s, \tag{89}$$

$$\|\mathbf{P}_1\| = -\|\mathbf{z}P_0\|, \tag{90}$$

$$\|\nabla\mathbf{P}_1\| = -\|\nabla(\mathbf{z}P_0)\|. \tag{91}$$

For $m = 1$, Eqs. (63) - (65) give

$$\frac{d\mathbf{M}_1}{dt} = -\int_{S_e} d\mathbf{S}\cdot\left(\|\mathbf{U}\mathbf{P}_1^{[1]}\| - D\|\nabla\mathbf{P}_1\|\right). \tag{92}$$

Substituting the boundary conditions (91) and (58) into this expression yields

$$\frac{d\mathbf{M}_1}{dt} = \int_{S_e} d\mathbf{S}\cdot\left(\|\mathbf{U}\mathbf{z}P_0^{[1]}\| - D\|\nabla(\mathbf{z}P_0)\|\right). \tag{93}$$

Use of (64) allows this to be written as

$$\frac{d\mathbf{M}_1}{dt} = \int_{\partial V} d\mathbf{S}\cdot\mathbf{U}\mathbf{z}P_0^{[1]} - D\int_{\partial V} d\mathbf{S}\cdot\nabla(\mathbf{z}P_0), \tag{94}$$

or, upon using the divergence theorem,

$$\begin{aligned}\frac{d\mathbf{M}_1}{dt} &= \int_V \nabla\cdot(\mathbf{U}\mathbf{z}P_0^{[1]}) - D\nabla\cdot\nabla(\mathbf{z}P_0)\, d^3\mathbf{r} \\ &= \int_V (\mathbf{U}\cdot\nabla P_0^{[1]} - D\nabla^2 P_0)\,\mathbf{z} + \mathbf{i}_z\left(U_z P_0^{[1]} - D\frac{\partial P_0}{\partial z}\right) d^3\mathbf{r},\end{aligned} \tag{95}$$

where $U_z = \mathbf{i}_z\cdot\mathbf{U}$, with $\mathbf{i}_z$ a unit vector in the z-direction. However, from (78), the gradient of $P_0^{[1]} \simeq \mathbf{0}$. Furthermore, for long times, $P_0 \simeq P_0^{\infty}$, so that as a consequence of (82), $\nabla^2 P_0^{\infty} \to 0$ for long times. Thus, we obtain

$$\frac{d\mathbf{M}_1}{dt} \simeq \overline{\mathbf{U}} M_0^{[1]} + \mathbf{A}^*, \tag{96}$$

where

$$\mathbf{A}^* = \mathbf{i}_z A^*, \tag{97a}$$

$$A^* = -D\int_V \frac{\partial P_0^{\infty}}{\partial z} d^3\mathbf{r}, \tag{97b}$$

and

$$\overline{\mathbf{U}} = \mathbf{i}_z \overline{U}, \tag{98a}$$

$$\overline{U} = \frac{1}{V}\int_V U_z d^3\mathbf{r}. \tag{98b}$$

The convective contribution in (96) may be written as

$$\mathbf{U}M_0^{[1]} = \mathbf{i}_z \sum_{n=0}^{\infty} 2^{-n} \overline{U} \int_V P^n dV. \tag{99}$$

Eqs. (5) and (7) combine to give

$$\overline{\mathbf{V}_n} = \frac{1}{V} \int_V 2^{-n} \mathbf{U}(\mathbf{r})\, d^3\mathbf{r}, \tag{100}$$

which is equivalent to

$$\overline{\mathbf{V}_n} = \mathbf{i}_z 2^{-n} \overline{U}. \tag{101}$$

Comparison of (99) and (101) reveals

$$\mathbf{U}M_0^{[1]} = \sum_{n=0}^{\infty} \overline{\mathbf{V}_n} \int_V P^n dV. \tag{102}$$

In words, this means that when the particle is in cell n, the convective contribution to the particle's velocity is equal to the average fluid velocity in that cell.

Integration of (96) with respect to time yields

$$\mathbf{M}_1 = \mathbf{U} \int M_0^{[1]} dt + \mathbf{A}^* t + \overline{\mathbf{B}}, \tag{103}$$

where the integral on the right-hand side of (103) is an indefinite integral and $\overline{\mathbf{B}}$ is an arbitrary position- and time-independent vector. The fact that the functional dependence of $M_0^{[1]}$ on time is explicitly unknown is irrelevant to the subsequent analysis. One needs only to seek a macrotransport equation whose first moment exhibits the same dependence on $M_0^{[1]}$.

We now seek an asymptotic trial solution for the $\mathbf{P}_1$ field. It will be verified *a posteriori* that insofar as dominant terms are concerned

$$\mathbf{P}_1 \simeq \mathbf{P}_1^{\infty} \tag{104}$$

where

$$\mathbf{P}_1^{\infty} = \left[\overline{\mathbf{U}}\int M_0^{[1]}\,dt + \mathbf{A}^* t + \mathbf{B}\right] P_0^{\infty}. \tag{105}$$

Here, $\mathbf{B}(\mathbf{r},t)$ is a vector field to be determined. Upon integrating (105) over the volume of the unit cell, substituting the relationship given by (86), and comparing the result with (103), it can be verified that the assumed solution for $\mathbf{P}_1^{\infty}$ guarantees that

$$\int_V \mathbf{P}_1^{\infty} d^3\mathbf{r} \simeq \mathbf{M}_1, \tag{106}$$

provided that $\overline{\mathbf{B}}$ is defined so that

$$\overline{\mathbf{B}} = \int_V \mathbf{B} P_0^{\infty} d^3\mathbf{r}. \tag{107}$$

2.3 Determination of the B Field

Substitute Eqs. (105) and (88) into (87) to obtain the following equation governing the **B** field:

$$\overline{\mathbf{U}} M_0^{[1]} P_0^{\infty} + \mathbf{A}^* P_0^{\infty} + \frac{\partial \mathbf{B}}{\partial t} P_0^{\infty} = -\mathbf{U}\cdot\nabla\mathbf{P}_1^{[1]} + D\nabla^2(\mathbf{B}P_0^{\infty}). \tag{108}$$

Substitute Eq. (105) into the boundary conditions (89) - (91) imposed on $\mathbf{P}_1$ and use Eqs. (83) - (85) to obtain the following boundary conditions required of the **B** field:

$$\mathbf{v}\cdot\nabla\mathbf{B} = 0 \quad \text{on } S_g, \tag{109}$$

$$\mathbf{B}(\mathbf{r}) = \mathbf{B}(\mathbf{r}+\mathbf{l}\pm\mathbf{h}) + \mathbf{l}, \tag{110}$$

$$\nabla\mathbf{B}(\mathbf{r}) = \nabla\mathbf{B}(\mathbf{r}+\mathbf{l}\pm\mathbf{h}). \tag{111}$$

Observe that although $\mathbf{B}$ is a function of time, $\bar{\mathbf{B}}$ is constant, consistent with the assumption made in (103). That this is so can be shown by integrating the governing equation for the $\mathbf{B}$ field over the volume of the unit cell.

The first term appearing on the right-hand side of Eq. (108) involves the $\mathbf{P}_1^{[1]}$ field, which has yet to be determined. The boundary-value problem for this field, determined by Eqs. (45), (46), (48), (58), and (59), is

$$\frac{\partial \mathbf{P}_1^{[1]}}{\partial t} + \mathbf{U}\cdot\nabla\mathbf{P}_1^{[2]} - \nabla^2\mathbf{P}_1^{[1]} = 0, \tag{112}$$

$$\mathbf{v}\cdot\nabla\mathbf{P}_1^{[1]} = 0 \quad \text{on } S_g, \tag{113}$$

$$\mathbf{P}_1^{[1]}(\mathbf{r}) = \mathbf{P}_1^{[1]}(\mathbf{r}+\mathbf{l}\pm\mathbf{h}) + \mathbf{l}P_0^{[1]}(\mathbf{r}), \tag{114}$$

$$\nabla\mathbf{P}_1^{[1]}(\mathbf{r}) = \nabla\mathbf{P}_1^{[1]}(\mathbf{r}+\mathbf{l}\pm\mathbf{h}), \tag{115}$$

where $\nabla P_0^{[1]}(\mathbf{r} + \mathbf{l} \pm \mathbf{h})$, which would have otherwise appeared in the latter expression was replaced by zero as a consequence of the asymptotic expression for $P_0^{[1]}$ (78). As shown in Appendix B, the boundary conditions represented by (114) and (115) imply that $\nabla\mathbf{P}_1^{[1]}$ is approximately equal to $M_0^{[1]}$. The solution to the macrotransport equation will show that $M_0^{[1]}$ decays rapidly with time (see Appendix C), so the terms $-\mathbf{U}\cdot\nabla\mathbf{P}_1^{[1]}$ and $\bar{\mathbf{U}}M_0^{[1]}P_0^{\infty}$ may be neglected relative to $\mathbf{A}^{*}P_0^{\infty}$. The result is therefore the following steady-state boundary-value problem for $\mathbf{B}$:

$$D\nabla^2(\mathbf{B}P_0^\infty) \simeq \mathbf{A}^* P_0^\infty, \tag{116}$$

$$\mathbf{v}\cdot\nabla\mathbf{B} = 0 \quad \text{on } S_g, \tag{117}$$

$$\mathbf{B}(\mathbf{r}) = \mathbf{B}(\mathbf{r}+\mathbf{l}\pm\mathbf{h}) + \mathbf{l}, \tag{118}$$

$$\nabla\mathbf{B}(\mathbf{r}) = \nabla\mathbf{B}(\mathbf{r}+\mathbf{l}\pm\mathbf{h}). \tag{119}$$

2.4 Second-Order Moments

Equations (63) - (65) with $m = 2$ combine to furnish the following expression:

$$\frac{d\mathbf{M}_2}{dt} = -\int_{S_e} d\mathbf{S}\cdot\left(\|\mathbf{U}\mathbf{P}_2^{[1]}\| - D\|\nabla\mathbf{P}_2\|\right). \tag{120}$$

The jump boundary conditions (55) and (60), allow this to be rewritten as

$$\frac{d\mathbf{M}_2}{dt} = \mathbf{I}_1 + \mathbf{I}_2, \tag{121}$$

wherein

$$\mathbf{I}_1 = -\int_{\partial V} d\mathbf{S}\cdot\mathbf{U}\left(\frac{\mathbf{P}_1^{[1]}\mathbf{P}_1^{[1]}}{P_0^{[1]}}\right), \tag{122}$$

and

$$\mathbf{I}_2 = D\int_{\partial V} d\mathbf{S}\cdot\nabla\left(\frac{\mathbf{P}_1\mathbf{P}_1}{P_0}\right). \tag{123}$$

On using the divergence theorem,

$$\mathbf{I}_2 = \int_V D\nabla^2\left(\frac{\mathbf{P}_1\mathbf{P}_1}{P_0}\right)d^3\mathbf{r}. \tag{124}$$

Into this equation, substitute the expression for $\mathbf{P}_1^\infty$ (Eq. (105)). Thus, asymptotically,

$$\mathbf{I}_2 \simeq D\int_V \nabla^2\left[(\bar{\mathbf{U}}g + \mathbf{A}^* t + \mathbf{B})^2 P_0^\infty\right]d^3\mathbf{r}, \tag{125}$$

where g is given by the indefinite integral

$$g=\int M_0^{[1]}\,dt. \tag{126}$$

Expand this expression and utilize the fact that $\nabla^2 P_0^\infty = 0$ to obtain

$$\mathbf{I}_2 \approx D\iint_V\left[(2\overline{\mathbf{U}}g + 2\mathbf{A}^*t)\nabla^2(\mathbf{B}P_0^\infty) + \nabla^2(\mathbf{B}\mathbf{B}P_0^\infty)\right]d^3\mathbf{r}. \tag{127}$$

Here, we have used the fact that the vectors **B**, $\mathbf{A}^*$, and **U** are all unidirectional in the z-direction so that **BU**=**UB** and $\mathbf{B}\mathbf{A}^*=\mathbf{A}^*\mathbf{B}$. Use the governing equation (116) for the **B** field to replace $D\nabla^2(\mathbf{B}P_0^\infty)$ in the above expression and expand $\nabla^2(\mathbf{B}\mathbf{B}P_0^\infty)$, thereby obtaining

$$\mathbf{I}_2 \approx 2(\overline{\mathbf{U}}g+\mathbf{A}^*t)\int_V \mathbf{A}^*P_0^\infty d^3\mathbf{r} + 2D\iint_V\left[\nabla(\mathbf{B}P_0^\infty)\mathbf{B} + P_0^\infty(\nabla\mathbf{B})^\dagger\cdot(\nabla\mathbf{B})\right]d^3\mathbf{r}. \tag{128}$$

Multiply Eq. (116) for the **B** field by **B** and substitute the resulting expression into the above equation. With use of (86), this gives

$$\mathbf{I}_2 \approx 2\mathbf{D}^* + 2\overline{\mathbf{U}}\mathbf{A}^*g + 2\mathbf{A}^*\mathbf{A}^*t + 2\mathbf{A}^*\overline{\mathbf{B}}, \tag{129}$$

in which

$$\begin{aligned}\mathbf{D}^* &= D\int_V P_0^\infty(\nabla\mathbf{B})^\dagger\cdot(\nabla\mathbf{B})\,d^3\mathbf{r}\\ &= \mathbf{i}_z\mathbf{i}_z D^*\ .\end{aligned} \tag{130}$$

Substituting the boundary condition (114) imposed on $\mathbf{P}_1^{[1]}$ into the expression for $\mathbf{I}_1$ (Eq. 122) gives

$$\mathbf{I}_1 = \int_{S_e} d\mathbf{S}\cdot\mathbf{U}(\mathbf{r}+\mathbf{l}\pm\mathbf{h})\left[2\mathbf{U}\mathbf{P}_1^{[1]}(\mathbf{r}+\mathbf{l}\pm\mathbf{h})\mathbf{l} + P_0^{[1]}(\mathbf{r}+\mathbf{l}\pm\mathbf{h})\mathbf{l}\mathbf{l}\right], \tag{131}$$

which may also be written as

$$\mathbf{I}_1 = \int_S d\mathbf{S}\cdot \bar{\mathbf{U}}\mathbf{z}\,(2\mathbf{P}_1^{[1]} + \mathbf{1}P_0^{[1]})\,, \tag{132}$$

(where the 'entrance' face of the cell has been taken to be $\mathbf{z} = \mathbf{0}$) or, using the divergence theorem:

$$\mathbf{I}_1 = \int_V \nabla\cdot\left[\bar{\mathbf{U}}\mathbf{z}\,(2\mathbf{P}_1^{[1]} + \mathbf{1}P_0^{[1]})\right]d^3\mathbf{r}\,. \tag{133}$$

Expand this expression and use the fact that $P_0^{[1]}$ is independent of position, together with the definitions of $M_0^{[1]}$ and $\mathbf{M}_1^{[1]}$. This eventually yields

$$\mathbf{I}_1 = 2\bar{\mathbf{U}}\mathbf{M}_1^{[1]} + \bar{\mathbf{U}}\mathbf{1}\mathbf{M}_0^{[1]} + 2\int_V \mathbf{U}\cdot(\nabla\mathbf{P}_1)\,\mathbf{z}\,d^3\mathbf{r} + \mathbf{i}_z 2\int_V U_z\,(\mathbf{P}_1 - \frac{\mathbf{M}_1^{[1]}}{V})\,d^3\mathbf{r}\,. \tag{134}$$

The time rate-of-change of the second centered moment may be expanded as

$$\frac{1}{2}\frac{d(\mathbf{M}_2 - \mathbf{M}_1\mathbf{M}_1)}{dt} = \frac{1}{2}\frac{d\mathbf{M}_2}{dt} - \mathbf{M}_1\frac{d\mathbf{M}_1}{dt}\,. \tag{135}$$

Substitute the expressions for $\mathbf{M}_1$ and the time rates-of-change of $\mathbf{M}_1$ and $\mathbf{M}_2$, given by Eqs. (96), (103), (121), (129), and (134) into this equation to obtain

$$\begin{aligned}\frac{1}{2}\frac{d(\mathbf{M}_2 - \mathbf{M}_1\mathbf{M}_1)}{dt} &\approx \mathbf{D}^* + \bar{\mathbf{U}}\,(\mathbf{M}_1^{[1]} - M_0^{[1]}\mathbf{M}_1) \\ &+ \frac{1}{2}\bar{\mathbf{U}}\mathbf{1}M_0^{[1]} + \mathbf{i}_z\int_V U_z\,(\mathbf{P}_1^{[1]} - \frac{\mathbf{M}_1^{[1]}}{V})\,d^3\mathbf{r} + \int_V \mathbf{U}\cdot\nabla\mathbf{P}_1^{[1]}\,\mathbf{z}\,d^3\mathbf{r}\,.\end{aligned} \tag{136}$$

It can be shown that each of the last three terms in the above expression is proportional to $\bar{U}M_0^{[1]}$ (See Appendix B). Thus, for long times, they may be neglected relative to the term $-\bar{\mathbf{U}}M_0^{[1]}\mathbf{M}_1$, because while $\mathbf{M}_1$ grows at least linearly with time, these terms are equal to $\bar{\mathbf{U}}M_0^{[1]}$ multiplied by a small constant. For long times, we therefore obtain

$$\frac{1}{2}\frac{d(\mathbf{M}_2 - \mathbf{M}_1\mathbf{M}_1)}{dt} \approx \mathbf{D}^* + \bar{\mathbf{U}}(\mathbf{M}_1^{[1]} - M_0^{[1]}\mathbf{M}_1) \ . \tag{137}$$

In the spatially periodic case (Brenner and Edwards (1993)), the above asymptotic expression for the second centered moment contains only $\mathbf{D}^*$, derived from the $\mathbf{B}$ field via Eq.(130). The additional term in the branching case results from the variation in the velocity in the axial direction. Its magnitude is always less than or equal to zero (for $\bar{U} > 0$) and thus results in a decrease in dispersion. This behavior can be understood by imagining a particle which diffuses backwards relative to the other particles. It will then diffuse into a region of higher velocity, which will tend to return it to its original position. Conversely, a particle which diffuses forwards will enter a region of lower velocity and will thus be moving more slowly than the rest of the particles, which will soon overtake it.

This 'extra' term is equal to zero in the case of a probability distribution which is a Dirac delta function. Under these conditions, the dispersivity is equal to $\mathbf{D}^*$, and the distribution will broaden. As it does so, however, the contribution to the dispersivity from the varying velocity becomes increasingly negative, decreasing the rate of dispersion. This type of behavior has also been observed by Delannay and Adler (1988) in their study of a branching system of stirred tanks. It is interesting to note that if the flow is in the opposite direction, towards the apex of the network, so that the velocity increases in the direction of flow, the opposite behavior is observed. Rather than decreasing the amount of dispersion, the varying velocity magnifies any dispersion which occurs, so that for long times, the time rate-of-change of the second centered moment becomes infinite.

3. THE MACROTRANSPORT EQUATION

In order to formulate a macrotransport description of transport through the branching network, it is necessary to find a macroscale equation whose moments asymptotically match those of the original, microscale problem. Subject to *a posteriori* verification, we assume this macrotransport equation to possess the following form:

$$\frac{\partial \bar{P}}{\partial t} + \frac{\bar{U}}{\bar{A}(Z)}\frac{\partial \bar{P}}{\partial Z} - \frac{D^*}{\bar{A}(Z)}\frac{\partial}{\partial Z}\left(\bar{A}(Z)\frac{\partial \bar{P}}{\partial Z}\right) = \delta(Z-Z')\,\delta(t)\,, \tag{138}$$

where the mean conditional probability $\bar{P}$ is defined in the range $0 < Z < \infty$ such that

$$\bar{A}(Z)\bar{P}(Z,t|Z') \sim \frac{1}{V}\int_V P^n(n,t|n',j',\mathbf{r}')\,d^3\mathbf{r} \qquad (\mathbf{i}_z Z = \mathbf{R}_n)\,, \tag{139}$$

where $\bar{A}(Z)$ is an average cross-sectional area, to be determined via the moment matching process. The area terms appearing in the third term of (138) result from the increasing area for diffusion.[1]

The macrotransport equation is to be solved subject to the following boundary conditions:

---

[1] This area dependence is analogous to that arising in the expansion of ∇^2 in non-Cartesian coordinate systems. For example, in the case of diffusion in a cylindrical wedge

$$\frac{\partial P}{\partial t} = D\left[\frac{1}{r}\frac{\partial}{\partial r}\left(r\frac{\partial P}{\partial r}\right) + \frac{\partial^2 P}{\partial \theta^2}\right].$$

Here, the cross-sectional area increases linearly with r.

$$\bar{J}(0,t) = 0, \tag{140}$$

$$\bar{P}(Z,t) \to 0 \quad \text{as } Z \to \infty, \tag{141}$$

where

$$\bar{J} = \frac{\bar{U}}{\bar{A}}\bar{P} - D^*\frac{\partial \bar{P}}{\partial Z}. \tag{142}$$

Define the moments of the mean conditional probability as

$$\bar{M}_m^{[\alpha]}(t|Z') = \int_0^\infty (Z-Z')^m \bar{P}\bar{A}^{(1-\alpha)}\,dZ. \tag{143}$$

This macroscale definition is meant to physically represent the microscale counterparts of the corresponding microscale definitions (42) and (44).

From (138), (143) and the boundary conditions (140) and (141), we find that for $\alpha = 0$

$$\bar{M}_0(t|Z') = \mathrm{H}(t). \tag{144}$$

Likewise,

$$\frac{d\bar{M}_1}{dt} = \bar{U}\bar{M}_0^{[1]} + D^*\frac{d\ln\bar{A}}{dZ}. \tag{145}$$

This expression for $\bar{M}_1$ will asymptotically match the comparable microscale expression (96) for M_1 provided that $\bar{A}$ is chosen such that

$$D^*\frac{d\ln\bar{A}}{dZ} = A^*, \tag{146}$$

where A^* is the constant defined in (97). Integration of the above expression gives

$$\bar{A} = \exp\left(\frac{A^*}{D^*}Z\right), \tag{147}$$

with the (arbitrary) cross-sectional area at $Z = 0$ taken to be unity.

From (138), (140) - (142), and (143) with m = 2 and $\alpha = 0$, it follows that

$$\frac{d\overline{M}_2}{dt} = 2D^* + 2D^* \frac{d\ln\overline{A}}{dZ}\overline{M_1} + 2\overline{UM_1}^{[1]} . \qquad \textbf{(148)}$$

Using Eqs. (145) and (148) yields

$$\frac{1}{2}\frac{d(\overline{M}_2 - \overline{M}_1\overline{M}_1)}{dt} = D^* + \overline{U}(\overline{M}_1^{[1]} - \overline{M}_0^{[1]}\overline{M}_1) \ . \qquad \textbf{(149)}$$

This macroscale expression asymptotically matches the corresponding microscale expression, Eq. (137). This macrotransport equation has the same moments as the microscale problem, and is thus an appropriate macrotransport equation.

III EXAMPLE: TRANSPORT IN A BRANCHING ARRAY

The boundary-value problems for the P_0^∞ and **B** fields defined by the systems of equations (82) - (86) and (116) - (119), respectively, were solved for a two-dimensional branching array such as that shown in Figure 3, using an implicit finite-difference method. Values for A^* and D^* were then calculated according to Eqs. (97) and (130). These results are plotted non-dimensionally in Figures 4 and 5 for various length-to-radius ratios (l/r) and branching-height-to-radius ratios (h/r), where the branching height, h, is measured from the centerline of the cell to the mid-point of the upper branch of the cell. Note that as the branching height increases, both A^*l/D and D^*/D decrease, a reflection of the increased distance that a particle must travel in the direction perpendicular to the axial direction in order to enter the next cell. Similarly, as l/r increases, both A^*l/D and D^*/D increase. For an h/r ratio of one, corresponding to the case of no separation between the

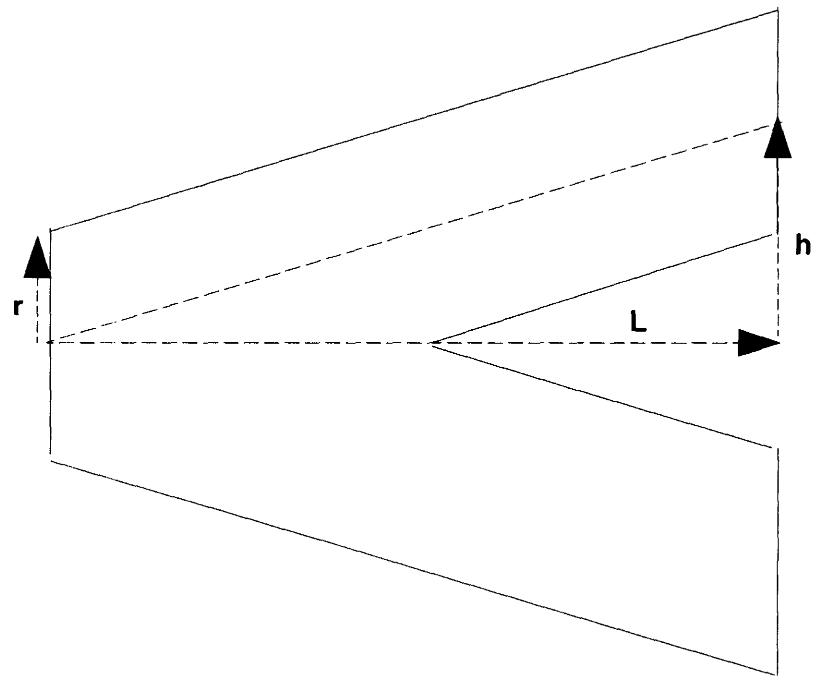

FIGURE 3: Two - Dimensional Branch Segment

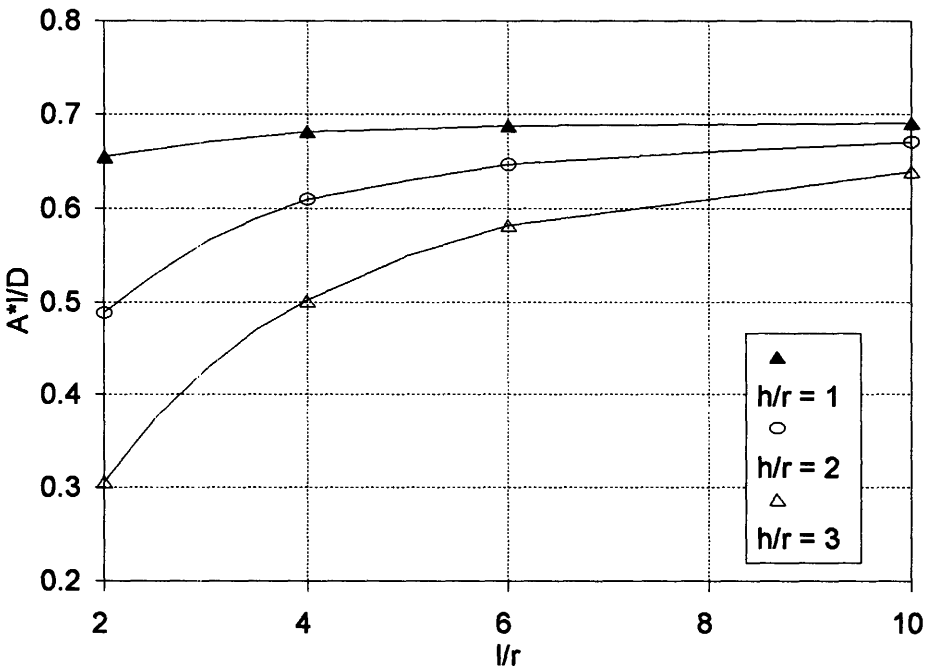

FIGURE 4: A*l/D

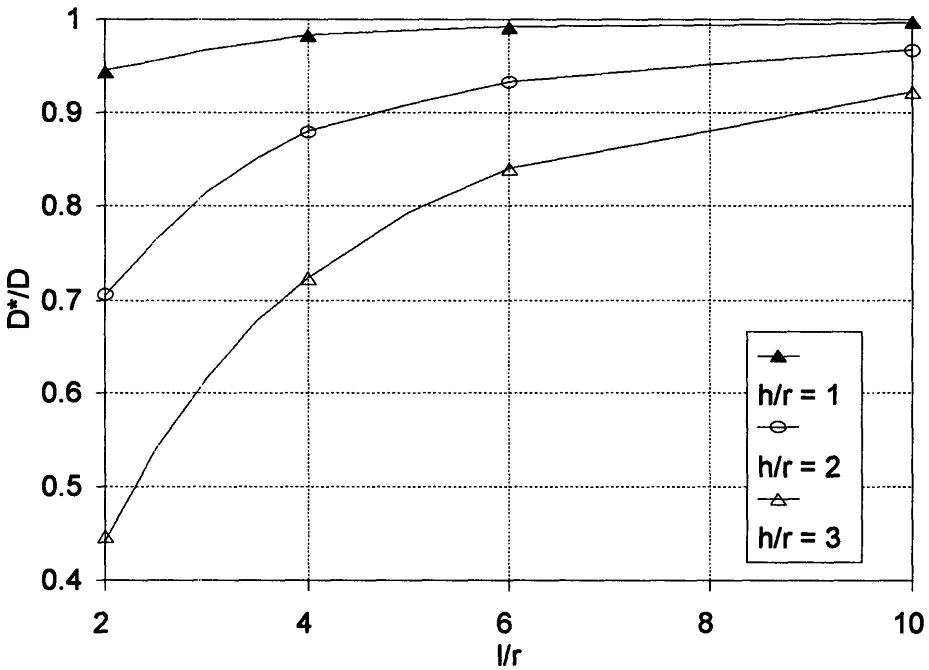

FIGURE 5: D*/D

two branches of the cell, A^*l/D and D^*/D asymptote to ln 2 and unity, respectively, as $l/r \to \infty$. These are the values they would assume in a continuously expanding system. For all values of l/r and h/r, the ratio A^*l/D^* is identically equal to ln 2, yielding

$$\overline{A}(z) = 2^{\frac{z}{l}}. \tag{150}$$

This is the value which would be expected for a system whose area doubles continuously every distance l.

For this example, the macrotransport equation becomes

$$\frac{\partial \overline{P}}{\partial t} + \frac{\overline{U}}{2^{\frac{z}{l}}}\frac{\partial \overline{P}}{\partial z} - \frac{D^*}{2^{\frac{z}{l}}}\frac{\partial}{\partial z}\left(2^{\frac{z}{l}}\frac{\partial \overline{P}}{\partial z}\right) = \delta(Z-Z')\,\delta(t). \tag{151}$$

This equation was solved numerically subject to the boundary conditions (140) and (141). Figures 6 and 7 illustrate the weighted probability distribution, $\overline{\overline{PA}}$, for Pe = 0.1 and 10, respectively, where Pe and T are defined in (72). Note that at Pe = 10, the distribution is more sharply peaked than at Pe = 0.1. This is due to the tendency for axial variations in velocity to decrease the dispersion. This phenomenon is further illustrated in Fig. 8 which compares the distributions after four diffusion times for the convective-diffusive cases, Pe = 10 and Pe = 0.1, and purely diffusive case, Pe = 0. In the convective-diffusive cases, there is a marked decrease in the net dispersion, this diminution increasing with increasing Peclet number. Observe that most of the decrease in the dispersion occurs in the high velocity region near the entrance to the system. In the low velocity region, Z/l >> 1, the differences between the probability distributions for various Peclet numbers are less pronounced.

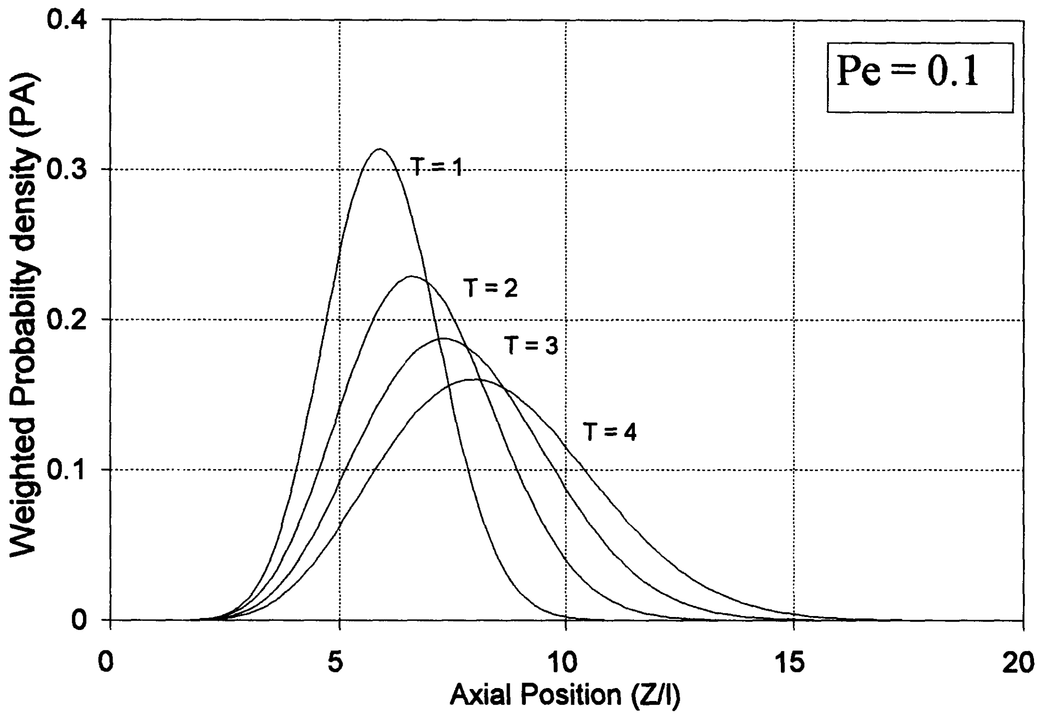

FIGURE 6: Probability Density (Pe=0.1)

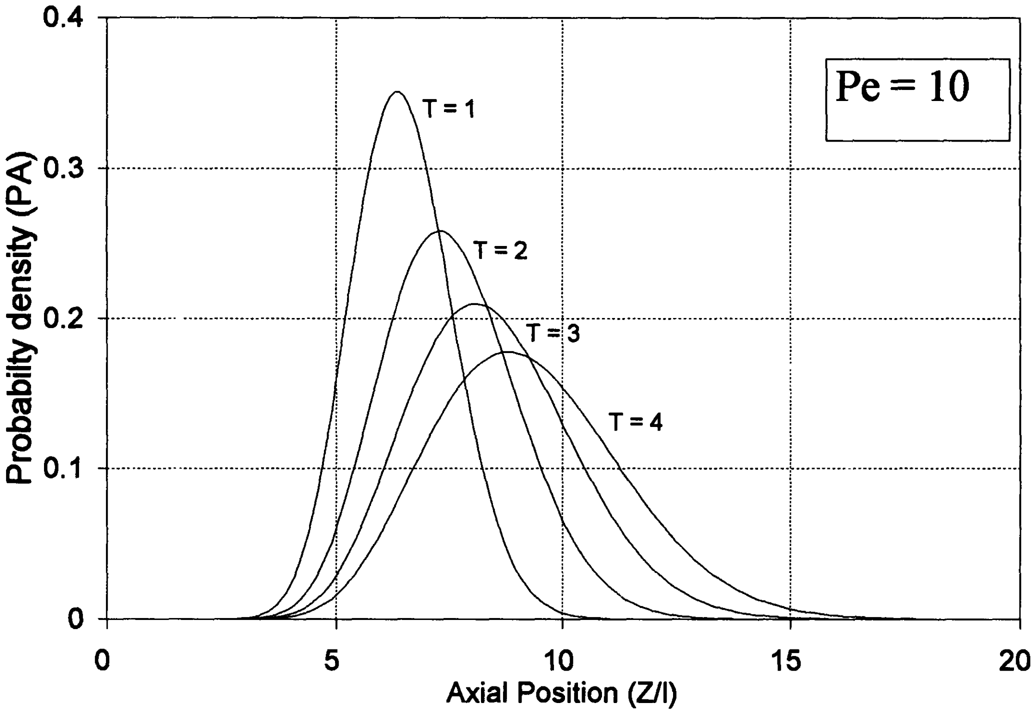

FIGURE 7: Probability Density (Pe=10)

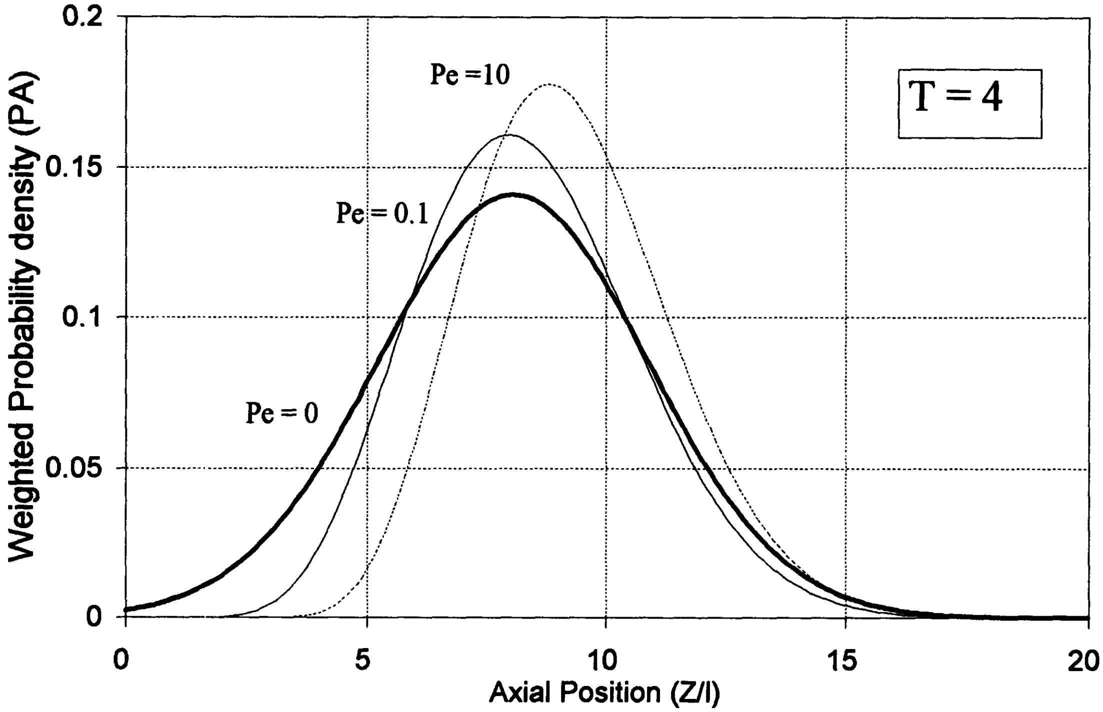

FIGURE 8: Probability Densities (T=4)

IV. CONCLUSIONS

Transport in a branching network is distinctly different from transport in a spatially periodic system due to the increasing area for diffusion and decreasing mean velocities in the direction of flow. Two phenomena present in a branching system which are not observed in spatially periodic systems were found. Firstly, the increasing cross-sectional area of the network results in a velocity-like effect caused by molecular diffusion, which is present even in the absence of convection. Secondly, axial dispersion is reduced as a consequence of the variation of the velocity in the axial direction. This reduction in dispersion increases monotonically with the Peclet number.

REFERENCES

Abramowitz, M. and Steegan, I.A. *Handbook of Mathematical Functions*. New York: Dover. (1965).

Bird, R. B., Stewart,W., and Lightfoot, E.N, *Transport Phenomena*. New York: John Wiley and Sons. p 559. (1960).

Brenner, H. and Edwards, D.A. *Macrotransport Processes*. Boston: Butterworth-Heinemann. Chapter 4. (1993).

Carslaw, H.S. and Jaegar, J.C. *Heat Conduction in Solids*. London: Oxford University Press. (1959).

Delannay, R.L. and Adler, P.M. Dispersion de Taylor dans une Structure Arborescente. *C.R. Acad. Sci. Paris*. **307**, 453-456. (1988).

Edwards, D.A. A General Theory of the Macrotransport of Nondepositing Particles in the Lung by Convective Dispersion I: General Theory. *J. Aerosol Sci.* (1994).

Federspiel, W.J. Analysis of Effective Axial Diffusion in Branching Networks. *AIChE Jour.* **38**, 1631-1638. (1992).

Ultman, J.S. and Blatman, H.S. A Compartmental Dispersion Model for the Analysis of Mixing in Tube Networks. *AIChE Jour.* **23**, 169-176. (1977).

APPENDIX A: DERIVATION OF JUMP BOUNDARY CONDITIONS

Zero-Order Moments

Sum Eq. (36) over all n and use the definition of P_0 (40) to obtain

$$P_0(\mathbf{r}+\mathbf{l}+\mathbf{h}) + P_0(\mathbf{r}+\mathbf{l}-\mathbf{h}) = P_0(\mathbf{r}) - P^0(\mathbf{r}) . \tag{A1}$$

This boundary condition involves the probability of the particle being at the inlet to the system, $P^0(\mathbf{r})$. By solving the macrotransport equation, it can be shown that for long times, $P^0(\mathbf{r})$ is negligible compared with $P_0(\mathbf{r})$ (See Appendix C). This term and other comparable terms are therefore systematically neglected throughout this paper in the long-time limit. The resulting boundary condition on P_0 is

$$P_0(\mathbf{r}+\mathbf{l}+\mathbf{h}) + P_0(\mathbf{r}+\mathbf{l}-\mathbf{h}) \approx P_0(\mathbf{r}) . \tag{A2}$$

A similar result may be derived from Eq. (37), namely

$$\nabla P_0(\mathbf{r}+\mathbf{l}+\mathbf{h}) + \nabla P_0(\mathbf{r}+\mathbf{l}-\mathbf{h}) \approx \nabla P_0(\mathbf{r}) . \tag{A3}$$

One can invoke symmetry arguments to show that $P_0(\mathbf{r}) = P_0(\mathbf{r}^*)$, where $\mathbf{r}^*$ is the point $\mathbf{r}$ reflected through the axis of symmetry. Through the use of this fact and the above relationships, it can be shown that $P_0(\mathbf{r}+\mathbf{l}+\mathbf{h}) = P_0(\mathbf{r}+\mathbf{l}-\mathbf{h})$. The above equations may therefore be written as

$$2P_0(\boldsymbol{r}+\boldsymbol{l}\pm\boldsymbol{h}) \approx P_0(\boldsymbol{r}) , \tag{A4}$$

$$2\nabla P_0(\boldsymbol{r}+\boldsymbol{l}\pm\boldsymbol{h}) \approx \nabla P_0(\boldsymbol{r}) . \tag{A5}$$

First-Order Moments

To derive the comparable boundary conditions imposed on the first moment, multiply (36) by $(\mathbf{R}_n - \mathbf{R}'_n)$ and sum over all n to get

$$2\mathbf{P}_1(\mathbf{r}+\mathbf{l}\pm\mathbf{h}) \simeq \mathbf{P}_1(\mathbf{r}) - \mathbf{l}P_0(\mathbf{r}) \,. \tag{A6}$$

Similarly

$$2\nabla\mathbf{P}_1(\mathbf{r}+\mathbf{l}\pm\mathbf{h}) \simeq \nabla\mathbf{P}_1(\mathbf{r}) - \mathbf{l}\nabla P_0(\mathbf{r}) \,. \tag{A7}$$

Add and subtract $\mathbf{z}P_0(\mathbf{r})$ on the right-hand side of (A6) (where $\mathbf{z}$ is the local axial coordinate) and use (A4) to derive an alternative form for (A6)):

$$2\mathbf{P}_1(\mathbf{r}+\mathbf{l}\pm\mathbf{h}) - \mathbf{P}_1(\mathbf{r}) \simeq -2(\mathbf{z}+\mathbf{l})P_0(\mathbf{r}+\mathbf{l}\pm\mathbf{h}) + \mathbf{z}P_0(\mathbf{r}) \,. \tag{A8}$$

Similarly, adding and subtracting $\mathbf{z}\nabla P_0(\mathbf{r})$ on the right-hand side of (A8) and using (A5) gives

$$2\nabla\mathbf{P}_1(\mathbf{r}+\mathbf{l}\pm\mathbf{h}) - \nabla\mathbf{P}_1(\mathbf{r}) \simeq -2(\mathbf{z}+\mathbf{l})\nabla P_0(\mathbf{r}+\mathbf{l}\pm\mathbf{h}) + \mathbf{z}\nabla P_0(\mathbf{r}) \,. \tag{A9}$$

Second-Order Moments

Following a similar procedure to that used to find the boundary conditions imposed on the first moments, multiply (36) by $(\mathbf{R}_n - \mathbf{R}'_n)^2$ and rearrange to obtain the following boundary conditions on $\mathbf{P}_2$:

$$2\mathbf{P}_2(\mathbf{r}+\mathbf{l}\pm\mathbf{h}) \simeq \mathbf{P}_2(\mathbf{r}) - 2\mathbf{l}\mathbf{P}_1(\mathbf{r}) + \mathbf{l}\mathbf{l}P_0(\mathbf{r}) \,, \tag{A10}$$

$$2\nabla\mathbf{P}_2(\mathbf{r}+\mathbf{l}\pm\mathbf{h}) \simeq \nabla\mathbf{P}_2(\mathbf{r}) - 2\mathbf{l}\nabla\mathbf{P}_1 + \mathbf{l}\mathbf{l}\nabla P_0(\mathbf{r}) \,. \tag{A11}$$

Use of (A4) - (A7) enables these boundary conditions to be rewritten as

$$2\mathbf{P}_2(\mathbf{r}+\mathbf{l}\pm\mathbf{h}) - \mathbf{P}_2(\mathbf{r}) \approx 2\frac{\mathbf{P}_1\mathbf{P}_1}{P_0}\bigg|_{\mathbf{r}+\mathbf{l}\pm\mathbf{h}} - \frac{\mathbf{P}_1\mathbf{P}_1}{P_0}\bigg|_{\mathbf{r}}, \tag{A12}$$

$$2\nabla\mathbf{P}_2(\mathbf{r}+\mathbf{l}\pm\mathbf{h}) - \nabla\mathbf{P}_2(\mathbf{r}) \approx 2\nabla\left(\frac{\mathbf{P}_1\mathbf{P}_1}{P_0}\right)\bigg|_{\mathbf{r}+\mathbf{l}\pm\mathbf{h}} - \nabla\left(\frac{\mathbf{P}_1\mathbf{P}_1}{P_0}\right)\bigg|_{\mathbf{r}}. \tag{A13}$$

$\alpha = 1$ Weighted Moments

To derive the boundary conditions imposed on the $\alpha = 1$ moments, proceed as with the unweighted moments, but multiply both sides of Eq. (36) by $2^{-n}(\mathbf{R}_n - \mathbf{R}'_n)^m$ before summing over all n. For the zeroth moment this yields

$$P_0^{[1]}(\mathbf{r}+\mathbf{l}\pm\mathbf{h}) \approx P_0^{[1]}(\mathbf{r}). \tag{A14}$$

As in the case of the unweighted moments, the term $P^0(\mathbf{r})$ has been neglected in the long-time limit relative to $P_0^{[1]}(\mathbf{r})$. Similarly,

$$\nabla P_0^{[1]}(\mathbf{r}+\mathbf{l}\pm\mathbf{h}) \approx \nabla P_0^{[1]}(\mathbf{r}). \tag{A15}$$

Analogously, for m = 1 and m=2, one obtains

$$\mathbf{P}_1^{[1]}(\mathbf{r}+\mathbf{l}\pm\mathbf{h}) \approx \mathbf{P}_1^{[1]}(\mathbf{r}) - \mathbf{l}P_0^{[1]}(\mathbf{r}), \tag{A16}$$

$$\nabla\mathbf{P}_1^{[1]}(\mathbf{r}+\mathbf{l}\pm\mathbf{h}) \approx \nabla\mathbf{P}_1^{[1]}(\mathbf{r}) - \mathbf{l}\nabla P_0^{[1]}(\mathbf{r}), \tag{A17}$$

$$\mathbf{P}_2^{[1]}(\mathbf{r}+\mathbf{l}\pm\mathbf{h}) \approx \mathbf{P}_2^{[1]}(\mathbf{r}) - 2\mathbf{l}\mathbf{P}_1{}^{[1]}(\mathbf{r}) + \mathbf{l}\mathbf{l}P_0^{[1]}(\mathbf{r}), \tag{A18}$$

$$\nabla\mathbf{P}_2^{[1]}(\mathbf{r}+\mathbf{l}\pm\mathbf{h}) \approx \nabla\mathbf{P}_2^{[1]}(\mathbf{r}) - 2\mathbf{l}\nabla\mathbf{P}_1{}^{[1]}(\mathbf{r}) + \mathbf{l}\mathbf{l}\nabla P_0^{[1]}(\mathbf{r}). \tag{A19}$$

Since the convective flux is given by $\mathbf{U}P^{[1]}$, it is convenient to multiply the boundary conditions on the weighted moments by $\mathbf{U}(\mathbf{r}) = 2\mathbf{U}(\mathbf{r} + \mathbf{l} \pm \mathbf{h})$. Eqs.(A14) - (A19) then become:

$$2\mathbf{U}(\mathbf{r}+\mathbf{l}\pm\mathbf{h})\,P_0^{[1]}(\mathbf{r}+\mathbf{l}\pm\mathbf{h}) \approx \mathbf{U}(\mathbf{r})\,P_0^{[1]}(\mathbf{r}), \tag{A20}$$

$$2\mathbf{U}(\mathbf{r}+\mathbf{l}\pm\mathbf{h})\,\nabla P_0^{[1]}(\mathbf{r}+\mathbf{l}\pm\mathbf{h}) \approx \mathbf{U}(\mathbf{r})\,\nabla P_0^{[1]}(\mathbf{r}), \tag{A21}$$

$$2\mathbf{U}(\mathbf{r}+\mathbf{l}\pm\mathbf{h})\,\mathbf{P}_1^{[1]}(\mathbf{r}+\mathbf{l}\pm\mathbf{h}) \approx \mathbf{U}(\mathbf{r})\,(\mathbf{P}_1^{[1]}(\mathbf{r}) - \mathbf{l}P_0^{[1]}(\mathbf{r})), \tag{A22}$$

$$2\mathbf{U}(\mathbf{r}+\mathbf{l}\pm\mathbf{h})\,\nabla\mathbf{P}_1^{[1]}(\mathbf{r}+\mathbf{l}\pm\mathbf{h}) \approx \mathbf{U}(\mathbf{r})\,(\nabla\mathbf{P}_1^{[1]}(\mathbf{r}) - \mathbf{l}\nabla P_0^{[1]}(\mathbf{r})), \tag{A23}$$

$$\begin{aligned}2\mathbf{U}(\mathbf{r}+\mathbf{l}\pm\mathbf{h})\,\mathbf{P}_2^{[1]}(\mathbf{r}+\mathbf{l}\pm\mathbf{h}) &\approx \\ \mathbf{U}(\mathbf{r})\,(\mathbf{P}_2^{[1]}(\mathbf{r}) &- 2\mathbf{l}\mathbf{P}_1^{[1]}(\mathbf{r}) + \mathbf{l}\mathbf{l}P_0^{[1]}(\mathbf{r})),\end{aligned} \tag{A24}$$

$$\begin{aligned}2\mathbf{U}(\mathbf{r}+\mathbf{l}\pm\mathbf{h})\,\nabla\mathbf{P}_2^{[1]}(\mathbf{r}+\mathbf{l}\pm\mathbf{h}) &\approx \\ \mathbf{U}(\mathbf{r})\,(\nabla\mathbf{P}_2^{[1]}(\mathbf{r}) &- 2\mathbf{l}\nabla\mathbf{P}_1^{[1]}(\mathbf{r}) + \mathbf{l}\mathbf{l}\nabla P_0^{[1]}(\mathbf{r})).\end{aligned} \tag{A25}$$

Jump Boundary Conditions

Define the 'branching jump' operator, $\| \ldots \|$ as the difference between the sum of the values of a function at a pair of equivalent points on the two exit faces of the cell and the value of this function at the equivalent point on the inlet face. Explicitly, for any scalar, vector, or tensor-valued function **f**,

$$\|\mathbf{f}\| \stackrel{def}{=} 2\mathbf{f}(\mathbf{r}+\mathbf{l}\pm\mathbf{h}) - \mathbf{f}(\mathbf{r}). \tag{A26}$$

The boundary conditions for both the $\alpha = 0$ and $\alpha = 1$ moments may be rewritten in terms of this operator. For the $\alpha = 0$ moments, one obtains:

$$\|P_0\| \approx 0, \tag{A27}$$

$$\|\nabla P_0\| \approx 0, \tag{A28}$$

$$\|\mathbf{P}_1\| \approx -\|\mathbf{z}P_0\|, \tag{A29}$$

$$\|\nabla\mathbf{P}_1\| \approx -\|\nabla(\mathbf{z}P_0)\|, \tag{A30}$$

$$\|\mathbf{P}_2\| \propto \left\| \frac{\mathbf{P}_1\mathbf{P}_1}{P_0} \right\|, \tag{A31}$$

$$\|\nabla\mathbf{P}_2\| \propto \left\| \nabla\left(\frac{\mathbf{P}_1\mathbf{P}_1}{P_0} \right) \right\|, \tag{A32}$$

whereas for $\alpha = 1$, the requisite jump boundary conditions are

$$\|\mathbf{U}P_0^{[1]}\| \propto 0, \tag{A33}$$

$$\|\mathbf{U}\nabla P_0^{[1]}\| \propto 0, \tag{A34}$$

$$\|\mathbf{U}\mathbf{P}_1^{[1]}\| \propto -\|\mathbf{U}\mathbf{z}P_0^{[1]}\|, \tag{A35}$$

$$\|\mathbf{U}\mathbf{P}_1^{[1]}\| \propto -\|\mathbf{U}\nabla(\mathbf{z}P_0^{[1]})\|, \tag{A36}$$

$$\|\mathbf{U}\mathbf{P}_2^{[1]}\| \propto \left\| \mathbf{U}\frac{\mathbf{P}_1^{[1]}\mathbf{P}_1^{[1]}}{P_0^{[1]}} \right\|, \tag{A37}$$

$$\|\mathbf{U}\mathbf{P}_2^{[1]}\| \propto \left\| \mathbf{U}\nabla\left(\frac{\mathbf{P}_1^{[1]}\mathbf{P}_1^{[1]}}{P_0^{[1]}} \right) \right\|. \tag{A38}$$

APPENDIX B: ESTIMATE FOR $\nabla \mathbf{P}_1^{[1]}$

Expand $\mathbf{P}_1^{[1]}$ in a Taylor series about the point $\mathbf{r}_m$, the point at which $\mathbf{P}_1^{[1]} = \mathbf{M}_1^{[1]}/V$:

$$\mathbf{P}_1^{[1]}(\mathbf{r}) = \mathbf{M}_1^{[1]}/V + (\mathbf{r} - \mathbf{r}_m)\cdot\nabla\mathbf{P}_1^{[1]}(\mathbf{r}_m) + (\mathbf{r} - \mathbf{r}_m)(\mathbf{r} - \mathbf{r}_m):\nabla\nabla\mathbf{P}_1^{[1]}(\mathbf{r}_m) + \ldots \tag{B1}$$

At either of the points $\mathbf{r} + \mathbf{l} \pm \mathbf{h}$

$$\mathbf{P}_1^{[1]}(\mathbf{r}+\mathbf{l}\pm\mathbf{h}) = \mathbf{M}_1^{[1]}/V + [(\mathbf{r}+\mathbf{l}\pm\mathbf{h}) - \mathbf{r}_m]\cdot\nabla\mathbf{P}_1^{[1]}(\mathbf{r}_m) + [(\mathbf{r}+\mathbf{l}\pm\mathbf{h}) - \mathbf{r}_m][(\mathbf{r}+\mathbf{l}\pm\mathbf{h}) - \mathbf{r}_m]:\nabla\nabla\mathbf{P}_1^{[1]}(\mathbf{r}_m) + \ldots \tag{B2}$$

Substitute these expansions into the boundary condition (110) to obtain

$$(\mathbf{r}-\mathbf{r}_m)\cdot\nabla\mathbf{P}_1^{[1]}(\mathbf{r}_m) = [(\mathbf{r}+\mathbf{l}\pm\mathbf{h})-\mathbf{r}_m]\cdot\nabla\mathbf{P}_1^{[1]}(\mathbf{r}_m) + \mathbf{l}P_0^{[1]}(\mathbf{r}) + O|\mathbf{r}-\mathbf{r}_m|^2, \tag{B3}$$

which eventually yields

$$(\mathbf{l}\pm\mathbf{h})\cdot\nabla\mathbf{P}_1^{[1]}(\mathbf{r}_m) = \mathbf{l}P_0^{[1]} + O|\mathbf{r}-\mathbf{r}_m|^2, \tag{B4}$$

or

$$\left.\left(l\frac{\partial\mathbf{P}_1^{[1]}}{\partial z} \pm h\frac{\partial\mathbf{P}_1^{[1]}}{\partial y}\right)\right|_{\mathbf{r}_m} = \mathbf{l}P_0^{[1]} + O|\mathbf{r}-\mathbf{r}_m|^2, \tag{B5}$$

where y is the coordinate in the direction of $\mathbf{h}$. In the above expression, the '±' allows one to conclude that in order for the expression to be valid with either the '+' or the '-', $\left.\frac{\partial\mathbf{P}_1^{[1]}}{\partial y}\right|_{\mathbf{r}_m} = 0$. Thus,

$$\nabla\mathbf{P}_1^{[1]} \approx \mathbf{i}_z\mathbf{i}_z P_0^{[1]} + O|\mathbf{r}-\mathbf{r}_m|^2. \tag{B6}$$

This estimate can be further refined by expanding $\nabla\mathbf{P}_1^{[1]}$ in a Taylor series about $\mathbf{r}_m$ to obtain

$$\nabla\mathbf{P}_1^{[1]}(\mathbf{r}) = \nabla\mathbf{P}_1^{[1]}(\mathbf{r}_m) + (\mathbf{r} - \mathbf{r}_m)\cdot\nabla\nabla\mathbf{P}_1^{[1]}(\mathbf{r}_m) + \mathrm{O}|\mathbf{r}-\mathbf{r}_m|^2. \tag{B7}$$

Substitute this expression into the boundary condition (115) and follow a procedure similar to that used above to show

$$\nabla\nabla\mathbf{P}_1^{[1]} \approx \mathrm{O}|\mathbf{r}-\mathbf{r}_m|^2. \tag{B8}$$

The third term in Eq. (B1) is therefore $\mathbf{O}|\mathbf{r} - \mathbf{r}_m|^4$ and the error estimate in (B6) may be replaced by $\mathbf{O}|\mathbf{r} - \mathbf{r}_m|^3$.

The estimate for $\mathbf{P}_1^{[1]}$ which is attained in this manner is

$$\mathbf{P}_1^{[1]}(\mathbf{r}) = \mathbf{M}_1^{[1]}/V + (\mathbf{r} - \mathbf{r}_m)\cdot\mathbf{i}_z\mathbf{i}_z P_0^{[1]} + \mathrm{O}|\mathbf{r}-\mathbf{r}_m|^3, \tag{B9}$$

from which it is clear that the second from last term in (136) is proportional to $M_0^{[1]}$, while (B6) shows that the same is true for the last term.

APPENDIX C: SOLUTION TO THE MACROTRANSPORT EQUATION AND VERIFICATION OF ASSUMPTIONS

Pe = 0 Solution

For Pe = 0, an analytical solution for the macrotransport equation (138) and boundary conditions ((140) - (141)) may be found. In order to utilize known solutions in one dimension, define a function $\Pi(Z,t)$ such that

$$\Pi(Z,t) = \overline{P}(Z,t)\, A_0 \exp(\lambda Z), \tag{C1}$$

where $\lambda = A^*/D^*$. Substituting this expression into the differential equation and boundary conditions for $\overline{P}$ gives the following problem in Π:

$$\frac{\partial \Pi}{\partial t} + D^* \lambda \frac{\partial \Pi}{\partial Z} - D^* \frac{\partial^2 \Pi}{\partial Z^2} = \delta(t)\,\delta(Z - Z'), \tag{C2}$$

$$\frac{\partial \Pi}{\partial Z} = \lambda \Pi \quad \text{at } Z = 0, \tag{C3}$$

$$\Pi \to 0 \quad \text{as} \quad Z \to \infty. \tag{C4}$$

This problem is normalized so that

$$\int_0^\infty \Pi \, dZ = 1. \tag{C5}$$

We now make the substitution

$$\Pi(Z,t) = u(Z,t) \exp\left(\frac{\lambda}{2}(Z - Z') - \frac{D^*}{4}\lambda^2 t\right). \tag{C6}$$

The resulting problem in u is

$$\frac{\partial u}{\partial t} = D^* \frac{\partial^2 u}{\partial Z^2} + \delta(t)\,\delta(Z-Z'), \tag{C7}$$

$$\frac{\partial u}{\partial Z} - \frac{\lambda}{2} u = 0 \quad \text{at} \quad Z = 0, \tag{C8}$$

$$u \to 0 \quad \text{as} \quad Z \to \infty. \tag{C9}$$

Carslaw and Jaeger (1959) give the solution to the diffusion equation with an instantaneous source at Z' and $\partial u/\partial Z = hu$ at $Z = 0$ as

$$u = \frac{1}{\sqrt{4\pi Dt}}\left(\exp\left(-\frac{(Z-Z')^2}{4Dt}\right) + \exp\left(-\frac{(Z+Z')^2}{4Dt}\right)\right) \\ - h\exp(Dth^2 + h(Z+Z'))\,\mathrm{erfc}\left(\frac{Z+Z'}{\sqrt{4Dt}} + h\sqrt{Dt}\right). \tag{C10}$$

In the present case, $h = \lambda/2$ and $D = D^*$. Back-substituting gives the following solution for $\bar{P}$:

$$\bar{P} = \frac{1}{A_0\sqrt{4\pi D^* t}}\left[\exp\left(-\frac{(Z-Z')^2}{4D^* t} - \frac{\lambda}{2}(Z+Z') - \frac{D^*}{4}\lambda^2 t\right) + \exp\left(-\frac{(Z+Z'+\lambda D^* t)^2}{4D^* t}\right)\right] \\ - \frac{\lambda}{2A_0}\,\mathrm{erfc}\left(\frac{Z+Z'}{\sqrt{4D^* t}} + \frac{\lambda}{2}\sqrt{D^* t}\right). \tag{C11}$$

For long times, this solution approaches

$$\bar{P} = \frac{1}{A_0\sqrt{\pi D^* t}}\exp\left(-\frac{D^*}{4}\lambda^2 t\right) - \frac{\lambda}{2A_0}\,\mathrm{erfc}\left(\frac{\lambda}{2}\sqrt{D^* t}\right). \tag{C12}$$

The limit as x approaches infinity of erfc(x) is

$$\mathrm{erfc}(x) \to \frac{\exp(-x^2)}{\sqrt{\pi}}\left(\frac{1}{x} - \frac{1}{x^3} + \frac{1\cdot 3}{2^2 x^5} + \cdots\right) \quad \text{as} \quad x \to \infty \tag{C13}$$

(Abramowitz and Steegan (1965)). Using this expression to approximate $\mathrm{erfc}\left(\frac{\lambda}{2}\sqrt{D^*t}\right)$ gives

$$\bar{P} \rightarrow \frac{2}{A_0\lambda^2\sqrt{\pi\,(Dt)^3}}\exp\left(-\frac{D^*}{4}\lambda^2 t\right) \qquad as \quad t \rightarrow \infty. \tag{C14}$$

Justification of Assumptions in Boundary Conditions

In order to justify neglecting the inlet condition in the boundary condition on P_0, we must compare the above expression with P_0. It has been shown that P_0 is conserved (Eq. (70)). Therefore, since $\bar{P}$ decays exponentially with time, $P^{(0,1)}(\mathbf{r})$ may be neglected relative to P_0. For Pe>0, no analytical solution exists. However, as the time-rate-of-change of the first moment increases with Pe, for a given time t, $P^{(0,1)}(\mathbf{r},t)$ decreases with increasing Pe, so it may be neglected relative to P_0 for all Pe.

Calculation of Weighted Moments and Verification of Assumptions in Equations for the B and $P_0^{[1]}$ Fields

The higher-order moments, $\bar{M}_0^{[\alpha]}$, may be calculated by multiplying the asymptotic solution (C12) for $\bar{P}$ by $\bar{A}^{(1-\alpha)}$ and integrating over all z. The $\alpha = 1$ total moment is

$$M_0^{[1]} \approx \frac{8\exp\left(-\frac{\lambda^2}{4}D^*t\right)}{A_0\lambda^3\sqrt{\pi\,(D^*t)^3}}, \tag{C15}$$

where the approximation for erfc(x) given above has been used. This moment decays exponentially with time, justifying the approximation made in (116).

For the $\alpha = 2$ moment, one obtains

$$M_0^{[2]} \approx \frac{20\exp\left(-\frac{\lambda^2}{4}D^*t\right)}{9A_0\lambda^3\sqrt{\pi\,(D^*t)^3}}. \qquad \text{(C16)}$$

We thus see that the ratio in (80) is 18/5 for Pe = 0. The ratio $\bar{M}_0^{[1]}/\bar{M}_0^{[2]}$ increases with increasing Pe, since as Pe increases, the probability distribution is shifted father downstream. Thus, from the solution for Pe = 0, one may conclude that for Pe << 18/5, the criterion in (80) is satisfied. For larger Pe, one must solve the macrotransport equation numerically and then verify the that (80) is satisfied. See Figure C1 for representative plots of $\bar{M}_0^{[1]}/\bar{M}_0^{[2]}$ versus time.

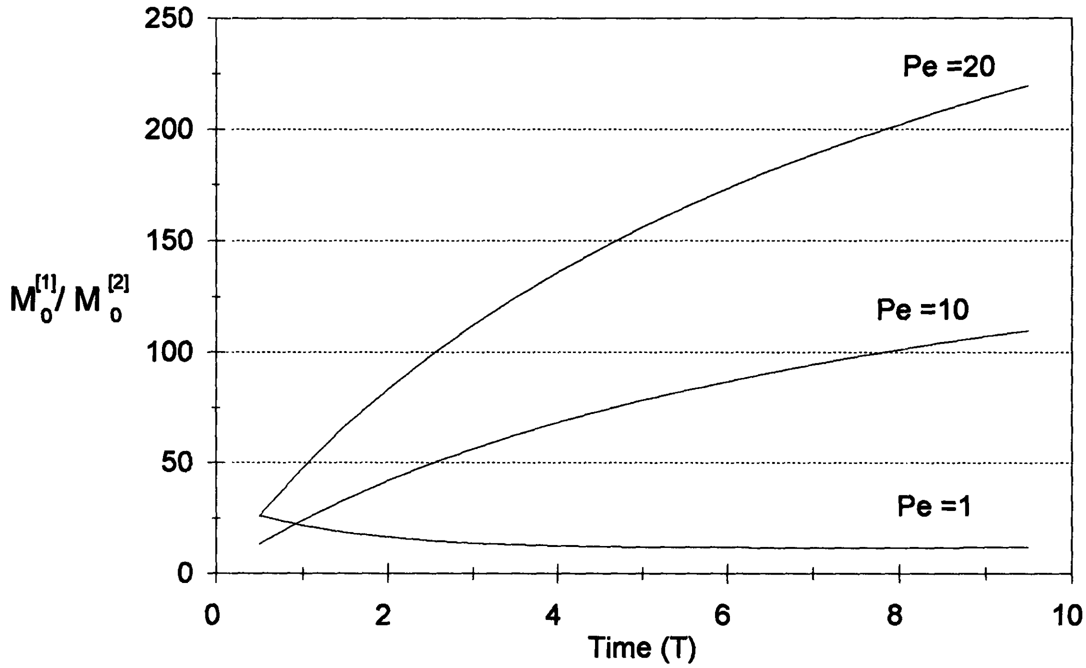

FIGURE C1: $M_0^{[1]}/ M_0^{[2]}$